Multi-indicator deterministic model based on time series of Sentinel-2, to assess the degree of natural succession on the abandoned arable areas

Małgorzata Kozak*, Anna Jędrejek, Rafał Pudełko

Department of Geomatics, Institute of Soil Science and Plant Cultivation – State Research Institute (IUNG-PIB),
24-100 Puławy, Poland; mkozak@iung.pulawy.pl, rpudelko@iung.pulawy.pl

***Correspondence author: e-mail: mkozak@iung.pulawy.pl; phone: +48 81 4786769

Abstract. The article presents the concept of a deterministic model for assessing the degree of natural succession on long-term abandoned land in the agricultural production area of Poland. The model was implemented as a geographic information system tool. It is based on two basic sources of information: cadastral maps, which can suggest if the agricultural land is agriculturally used, and seasonal time series of satellite images. The following working hypothesis was adopted in this study: "based on the data from the Sentinel-2 sensor, it is possible to assess the degree of natural succession on small and medium agricultural plots – by separating at least three classes of land cover, representing: early succession consisting mainly grass and ruderal vegetation, advanced succession represented by complexes of shrubs and young trees, mature succession - which is a transitional phase preceding the afforestation phase, or can already be a functional forest area". The obtained results confirmed the above hypothesis. In the case of early succession, the classification efficiency was about 94% in the winter period, for advanced succession about 75% in the autumn period, and for mature succession about 78% in the summer period. In the classification process, 8 vegetation indices were examined. In the end, the model algorithms were based on the GNDVI index, whose properties allowed for the best differentiation between the above-mentioned succession classes. NDVI, NDRE, NDVIre1, NDVIre2, NDVIre3 were used as auxiliary indices, which, as shown in the research, can improve the classification accuracy at a higher uncertainty threshold in case of weaker separation of classes with the GNDVI index.

Keywords: Sentinel-2 classification model; abandoned arable land, landuse change, natural succession

1. INTRODUCTION

The problem of agricultural land abandonment is still present in the ongoing changes in land cover and land use that can be observed in many parts of the world. This process has a particular bearing on Central and Eastern Europe. It is associated to the political transformations that began in the 1990s, after the collapse of the USSR and the bloc of satellite countries dependent on it. It resulted in a profound transformation of the functioning of economies in these regions, which also affected the agriculture of the countries (Janus, Bożek, 2019). Despite the passage of three decades, the effects of the conversion from centralized economy to free market economy are still visible in the agricultural area, additionally shaped by the EU's Common Agricultural Policy (CAP) (CAP 2023-27 – European Commission, 2024). As a direct consequence of these changes, now there is a high percentage of abandoned land in many European regions after the political transformation. This is especially true of southern, central and eastern Poland, where small farms survived the period of collectivization (Pudełko et al., 2018). After the political changes, in some of these farms production ceased to be economically viable (Collier, 2018). The first visible effect of land abandonment is the emergence of natural and invasive vegetation through secondary succession, which can

have a significant impact on the environment and landscape (Kozak, Pudełko, 2021; Lasanta et al., 2015). Plant succession usually occurs through the sequential appearance of new plant species in the area, gradually taking over the land (Falińska, 1997; Sosnowska, 2019). In the first stage of succession, segetal plants are the pioneer species to enter the abandoned agricultural land. In subsequent stages, vegetation of higher floors (shrubs, then trees) appears, and finally, after several years or decades, secondary afforestation takes place. Abandoned land is a broad definition that includes land that remains registered as agricultural land but is not in agricultural use. It can include, among other things, marginal land, but also fallow land. According to the definition of Anguiano et al. (2008) and Elbersen et al. (2014), the beginning of the fallowing process on agricultural land is identified when the land stays (agriculturally) unused for several years -at least two or five, depending on the definition.

In addition to issues relating to the causes of land abandonment, the effective use of the potential of such areas gained importance in recent years (Suziedelyte Visockiene et al., 2019). In order to manage effectively abandoned areas at the national and local level, it is essential to identify and record fallow land regionally, assess the state of plant succession and plan the future development of this type of agricultural plots. Development plans are usually shaped by strategies that guide and support, also financially, local initiatives. In the case of fallow lands, possible conversion scenarios for these areas are: restoration to agricultural production, afforestation, or protection as valuable natural or semi-natural habitats. Most of these forms of conversion are financially supported by the EU's CAP, under the so-called greening or now included in the Strategic Programme (*Eco-Schemes – European Commission*, 2024). The most radical form of landuse change is exclusion of land from agricultural production, allowing for introduction of industrial, communication or housing infrastructure (Stuczynski et al., 2009). Another interesting form of fallow land management is production of biomass for energy or industrial purposes. In this case, it is possible to eventually establish biomass plantations or restore the abandoned land to agricultural production by harvesting biomass from plots with advanced plant succession for profit (Matyka, Radzikowski, 2020; Stolarski et al., 2019; Stolarski et al., 2015). The EU policy also supports the introduction of renewable energy sources (RES) infrastructure in such areas (Directive – 2018/2001 – EN – EUR-Lex, n.d.).

When analyzing issues related to abandoned agricultural land, it is important to look into the potential methods of identifying such areas. In relation to other forms of landuse, statistical or cadastral data are not always available or up-to-date since farmers are not obliged to register all types of agricultural production. Therefore, it is easier to identify fallow land as agricultural land that is not registered for subsidies under the CAP (Pudełko et al., 2018).

However, this method is often unreliable, as it cannot guarantee that no plant production is carried out on agricultural plots – such as, for instance, biomass production for energy purposes, which is not covered by direct payments (Stolarski et al., 2020). Owing to that, the most reliable source of data at our disposal, which can provide information on the actual situation, is satellite imagery data.

In environmental remote sensing, including tracking the dynamics of agricultural land abandonment over long periods of time, images from Landsat satellites are the most commonly used. These data, thanks to their medium spatial resolution (30–40 m) and the free access to the archive (even from the 1970s), make it possible to monitor landuse changes in larger areas and for long time series (Dara et al., 2018; Grădinaru et al., 2019; Gutman, Radeloff, 2017; Yin et al., 2018). In Poland, Landsat images were used to estimate trends and perform segmentation (LU thematic classification) in the years 1986–2019. The research was carried out to identify periods of long-term greening and cross-reference them with the actual information on fallowing. However, as the authors admit, questions regarding the exact estimates and distribution of abandoned farms in Poland remain unanswered at present due to the complex nature of the phenomenon (Kolecka, 2021). The possibility of analyzing long-term changes in agricultural land use, especially in very large areas, on a national or even continental scale, is provided by satellite images with medium spatial resolution. An example of possible applications are products with a resolution of 250–1000 m from the MODIS image package and processed products. They were used, for example, to map abandoned land on a European scale, using the Normalized Diversified Vegetation Index (NDVI) time series. In this case, however, the greatest limitation is the spatial resolution, which, although it provides great freedom in the analysis of larger and compact areas, prevents the identification of dynamics on the scale of separate agricultural plots. (Estel et al., 2015; Zhu et al., 2021).

Since the middle of the second decade of the 21st century, high-resolution satellite images have been made available under the Copernicus program by the European Space Agency (ESA), which allowed for detailed analyses of the dynamics of changes in the use of agricultural land. For the above-mentioned purposes, the data obtained by multispectral Sentinel-2 sensors seem to be the most useful (Sentinel-2, n.d.). Imaging in the range of green, red, red-edge and infrared radiation is ultimately dedicated to the monitoring of vegetation cover, and image resolution (10–20 m) allows for analyzing imaging within the boundaries of most agricultural plots, in the case of Poland, or clusters of small plots which are subject to similar fallowing processes – this phenomenon is often observed in the southern and eastern regions of the country (Kolecka et al., 2017; Sosnowska, 2019). An example of research in very fragmented agricultural landscapes, e.g. the Polish

Carpathians is the use of high-resolution remote sensing data such as: airborne laser scanning – ALS, LiDAR – light detection and ranging, point clouds or from fine resolution aerial photographs. The above-mentioned data sets make it possible to assess the amount of natural succession, and thus, indirectly draw conclusions about the time of cessation of agricultural land use (Jabs-Sobocińska et al., 2021; Kolecka, 2018; Kolecka, Kozak, 2019; Shahbandeh et al., 2022). The main barrier to the use of Sentinel-2 images is the too short period of the time series for archival images, which is a significant limitation to conducting research on the dynamics of long-term landuse changes. Therefore, there is a need to supplement the data on the situation from before 2015/16 by analyzing other archival data, mainly the Landsat images mentioned above. In Poland, aerial photographs are also available, which have been taken regularly since the mid-1990s for the purposes of building a cadastral system in regional administration and Land Parcel Identification System (LPIS) (geoportal.gov.pl, n.d.; Trystuła, Konieczna, 2008). These data allow for identifying the exact dates of abandonment of agricultural production on the monitored plots, which is also the starting date of the natural succession processes (Kozak, Pudełko, 2021; Szostak et al., 2018).

In addition to the opportunities in acquiring multispectral data, methods and approaches to land use classification have developed in parallel, including in the context of identifying unused land. Many publications on the subject have used Object-Based Image Analysis (OBIA) to identify abandoned agricultural land. OBIA is an automatic classification method that uses image objects as the basic units instead of individual pixels, the method is based on segmentation, which groups pixels into shapes that represent individual objects (Goga et al., 2019; Jabs-Sobocińska et al., 2021; Suziedelyte Visockiene et al., 2019; Szostak et al., 2016, 2018; Toure et al., 2018; Yusoff et al., 2017). Despite the very good results, the downside of this method is the need for specialized software and time-consuming when segmenting larger areas. In contrast, pixel-based classification still appears to be a versatile approach, with a range of available classification algorithms.

Recently, a widely used method is the use of machine learning algorithms, such as Support Vector Machines – SVM, Nearest Neighbor – NN, random forests – RF and classification trees – CT, supported by regression models or phenological aspects (Abdi, 2020; Macintyre et al., 2020; Morell-Monzó et al., 2020). The machine learning approach provides ample opportunities to capture multiple variables, handle multivariate data but also model nonlinear relationships (Alonso et al., 2015). When identifying abandoned agricultural land, natural succession or classifying vegetation types, the most popular methods use vegetation indices mainly NDVI and its derivatives as well as EVI, GNDVI, SAVI but also many combinations of spectral bands, including e.g. SWIR or Red Edge bands avail-

able to Sentinel 2 (Goga et al., 2019; Hawryło et al., 2018; Macintyre et al., 2020; Morell-Monzó et al., 2020). The listed vegetation indices are often compiled into multi-time series, using which it is possible to capture phenological differences between vegetation classes and determine the optimal time of data acquisition (Tumelienė et al., 2021). Since each region is characterized by specific vegetation types and the course of the phenological period, most studies concern the local scale. Indicating the best term for identifying abandoned areas will therefore depend on the specifics of the region and the methodological approach. For example, Tumelienė et al. (2021) showed that the best date for identifying abandoned areas for the Lithuanian area, was autumn – September, while in the case stage for Slovakia, the best date was July (Szatmári et al., 2018; Tumelienė et al., 2021).

The main purpose of this article is to answer the question to what extent mid-resolution and multi-spectral satellite imagery can be used to assess the degree of natural succession on abandoned agricultural land. The key assumption formulated by the research group is to develop a universal model that will allow for the assessment and classification of the progress of the natural succession, which, in the future, is to be incorporated into the decision support system regarding the strategy of fallow land and wasteland management as well as obtaining biomass and developing renewable energy sources in rural areas.

The authors put forward the following working hypothesis – based on the Sentinel-2 satellite images, it is possible to assess the degree of natural succession on small and dispersed agricultural plots by separating at least three land cover classes, which represent: (1) early succession, represented mainly by ruderal vegetation; (2) advanced succession, represented by complexes of shrubs and young trees; (3) mature succession – a transitional phase that takes place just before the afforestation, or may constitute a functional forest area.

2. MATERIALS AND METHODS

2.1. Study area

The research area is located in southeastern Poland. It covers part of the Puławy commune, which is a Local Administrative Unit (LAU code:1006061121409) according to the Eurostat nomenclature, located in the northwestern part of the Lubelskie Voivodeship (NUTS-2: PL81) – Figure 1. The area is located on the left bank of the Vistula River. It is a coherent region in terms of functionality, which until the 1990s, i.e. the beginning of the political changes that led to the described landuse changes, was characterised mainly by agricultural activity. Despite the growing pressure of housing development and the outflow of rural population, the area has not lost its agricultural character, and its proximity to the city of Puławy (the capital of the
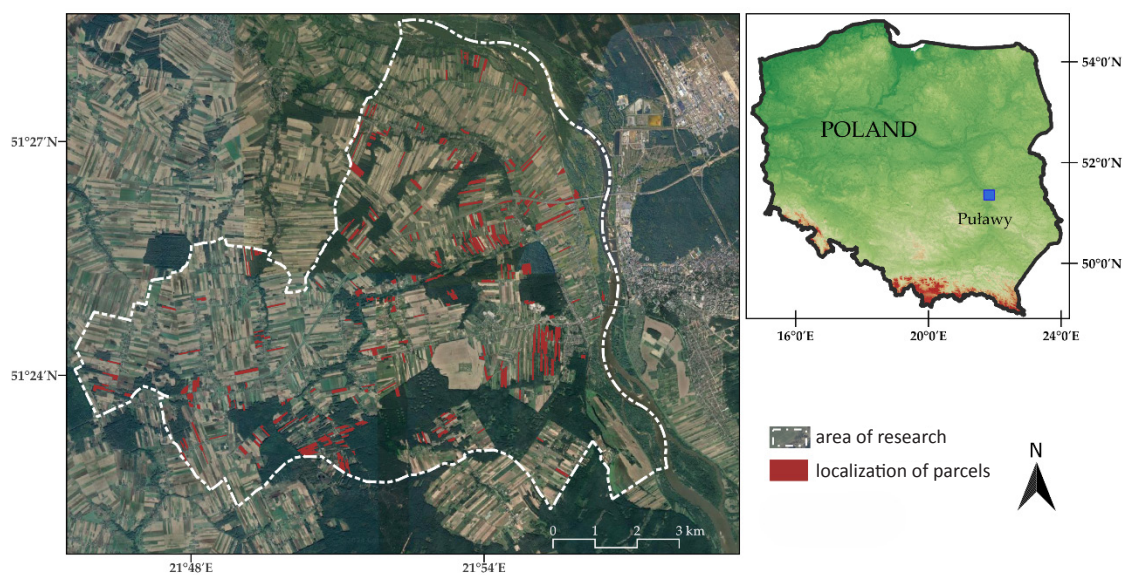
Figure 1. Location of the study area. Own study.

region) makes it a food production base. In the study area, the sowing structure is dominated by cereal crops (about 45%) mainly winter wheat and winter triticale, a large percentage is also occupied by permanent crops such as orchards or plantations of strawberries, blueberries. The specificity of the agricultural area of the region is the large fragmentation of farms and small size of individual agricultural plots, which, to some extent, could determine the emergence of abandoned land in the landscape ('Study of conditions and directions of spatial development', n.d.)

2.2. Data Sources

2.2.1. Location of the potentially abandoned agricultural land

In order to locate potentially abandoned land, cadastral plots not declared for direct payments (under the CAP) and at the same time having the attributes of agricultural land (arable land, meadows, pastures) were selected. The LPIS database administered by The Agency for Restructuring and Modernisation of Agriculture (ARMA) was used for identification. The WMS layer of land cover objects was downloaded from the public server (current status as of 2021.11.23) – preview available on the national geoportal: mapy.geoportal.gov.pl (*geoportal.gov.pl*, n.d.). The fact that farmers do not apply for direct payments for the selected parcels can prove that there is no plant production on these plots, i.e. that they are agriculturally abandoned.

2.2.2. Remote Sensing data

The next step in our study was to acquire and prepare satellite images. The research was based on images provided by ESA (The European Space Agency) from the Co-

pernicus Sentinel-2 (S-2) mission. The mission is based on a constellation of two twin satellites orbiting on the same path. Each satellite is equipped with a multispectral imaging system with 13 spectral bands, offering a high-resolution spatial image registration (10 m, 20 m or 60 m). Each S-2 sensor provides a 10-day revisit period, which, with combination of Sentinel-2A and Sentinel-2B satellites, is reduced to 5 days (Sentinel-2, n.d.).

The analysis of time series in the assumed scenario required the acquisition of all possible S-2 optical images produced throughout the growing season. For the study area, 14 almost cloudless images from the year 2019 were obtained (Table 1).

Table 1. Sentinel-2 acquisitions.

Date of satellite pass	Scene id
2019-02-19	L2A_T34UEC_A010215_20190219T094304
2019-03-31	L2A_T34UEC_A010787_20190331T094033
2019-04-15	L2A_T34UEC_A019910_20190415T094033
2019-04-25	L2A_T34UEC_A020053_20190425T094505
2019-06-09	L2A_T34UEC_A011788_20190609T094208
2019-06-14	L2A_T34UEC_A020768_20190614T094034
2019-07-29	L2A_T34UEC_A012503_20190729T094242
2019-08-28	L2A_T34UEC_A012932_20190828T094520
2019-09-22	L2A_T34UEC_A022198_20190922T094031
2019-10-12	L2A_T34UEC_A022484_20191012T094345
2019-10-27	L2A_T34UEC_A013790_20191027T094607
2019-11-01	L2A_T34UEC_A022770_20191101T094343
2019-11-16	L2A_T34UEC_A014076_20191116T094318
2019-12-06	L2A_T34UEC_A014362_20191206T094328

Then, for each acquisition date, a series of vegetation indices (VI) were generated. The following assumptions were made when selecting indicators:

– No more than 10 types of indices will be tested;
– Tested indicators should be based on the band ranges dedicated to remote sensing of vegetation (Bands 3–8 see Table 2);
– Spatial resolutions of 10 m will be preferred.

In the end, eight vegetation indices were selected to assess the degree of natural succession (Table 3). It should be noted that three of the selected indicators are modifications of the NDVI index (NDVIre1, NDVIre2, NDVIre3), taking into account the red edge ranges (spectral bands: 5, 6, and 7) instead of the standard near infrared (NIR, band 8). Such a combination of bands, including a 10 m resolution visible Red band, was supposed to make the NDVI index more sensitive to narrow red edge bands, without sacrificing the spatial resolution. The selection of vegetation indices was based on a literature review.

In the next step, eight vegetation index (VI) maps were generated for all S-2 images listed in Table 1. The entire process of image data processing (downloading from the ESA server, trimming to the boundaries of the study area, initial processing of satellite images including atmospheric correction, calculation of spectral indices and resampling to a 10 m resolution) was performed in the R environment using the sen2r package (Ranghetti et al., 2020).

2.3. Methods

The study was carried out in the following sequential steps: verification and generalization of the database of agricultural plots selected for analysis (section 2.3.1.); determination of spectral signatures for pre-defined succession classes (section 2.3.2.); development of satellite data VI statistics (section 2.3.3); identification of the best observation periods for LU classification (section 2.3.4), development of a classification model and assessment of its accuracy (section 2.3.5, 2.3.6).

Table 2. The spectral and spatial resolution of Sentinel-2's bands.

Sentinel-2 Bands	Resolution [m]	Central Wavelenght [µm]
Band 2 (b2) – Blue	10	0.490
Band 3 (b3) – Green	10	0.560
Band 4 (b4) – Red	10	0.665
Band 5 (b5) – Vegetation Red Edge1	20	0.705
Band 6 (b6) – Vegetation Red Edge2	20	0.740
Band 7 (b7) – Vegetation Red Edge3	20	0.783
Band 8 (b8) – NIR	10	0.842
Band 8a (b8a) – Vegetation Red Edge4	20	0.865
Band 11 – SWIR	20	1.610
Band 12 – SWIR	20	2.190

Source: https://sentinel.esa.int/web/sentinel/user-guides/sentinel-2-msi/resolutions/spatial

Table 3. List of explored spectral indices of vegetation.

Vegetation index	Equation for S2 bands	Reference
NDVI Normalized Difference Vegetation Index	$\dfrac{b8 - b4}{b8 + b4}$	Rouse et al., 1974
GNDVI Green Normalized Difference Vegetation Index	$\dfrac{b8 - b3}{b8 + b3}$	Gitelson, Merzlyak, 1998
EVI Enhanced Vegetation Index	$2.5 \dfrac{b8 - b4}{b8 + 6b4 - 7.5}$	Huete et al., 2002
SAVI Soil Adjusted Vegetation Index	$\dfrac{1.5 * b8 - b4}{b8 + b4 + 0.5}$	Huete, 1988
NDVIre1 Red-edge1 Normalized Difference Vegetation Index	$\dfrac{b5 - b4}{b5 + b4}$	Hansen, Schjoerring, 2003; Herrmann et al., 2011; *IDB - Index DataBase*, n.d.; Thompson et al., 2019
NDVIre2 Red-edge1 Normalized Difference Vegetation Index	$\dfrac{b6 - b4}{b6 + b4}$	
NDVIre3 Red-edge1 Normalized Difference Vegetation Index	$\dfrac{b7 - b4}{b7 + b4}$	
NDRE Normalized Difference Red Edge	$\dfrac{b8 - b5}{b8 + b5}$	Barnes et al., 2000

2.3.1. Preparation of ground data (agricultural plots)

The obtained database of undeclared agricultural parcels (as described in section 2.2.1) was prepared for further analysis in the following steps:

• Plots with an area of less than 0.3 ha were removed from the database, except when they constituted a complex of plots – then, they were merged (Figure 2). The purpose of this pre-selection process was to exclude objects which were too small for remote sensing with S-2 resolution.

• Verification of the actual fallowing/land abandonment was carried out – by eliminating plots that are still cultivated or subject to conversion for non-agricultural purposes (buildings, infrastructure). In order to confirm the

Figure 2. A: an example of a complex of small agricultural plots directly adjacent to each other; B: polygon created by connecting the plots – generated for further analyses using remote sensing methods.

abandonment status and determine the approximate date of abandonment from agricultural production, verification was carried out based on the current and historical orthophotomaps from the period of 1997–2020 provided by GUGIK – The Head Office of Geodesy and Cartography (*geoportal.gov.pl*, n.d.). All such verified plots were then personally inspected in-situ.

2.3.2. Scheme for determining spatial signatures

Referring to earlier research conducted in this area (Kozak, Pudełko, 2021) – natural succession was divided into three main classes of land cover:

– Class 1 – Goldenrod – areas with a predominance of plants of later succession stages, mainly goldenrod (*Solidago* L.), tansy (*Tanacetum vulgare* L.). Criterion: Over 80% share of goldenrod or tansy in land cover.

– Class 2 – Bushy – areas where apart from ruderal plants, such as goldenrod (*Solidago* L.), there are bushes, e.g., in the form of blackberries (*Rubus* L.), blackthorn (*Prunus spinosa* L.) and single self-seeded trees. Criterion: Over 30% share of bushes in land cover.

– Class 3 – Wooded/afforested – areas with trees, dense shrubs, advanced succession. Criterion: places where young forest covered at least 0.10 ha.

When determining ground reference data, the fact that individual classes of natural succession are characterized by high diversity even within a single pixel, as well as the uncertainty of delineated boundaries between these classes, was taken into account. Therefore, instead of points, polygons were determined, each containing at least 9 pixels, with a resolution of 10 m × 10 m – in line with the resolution of the four basic S-2 channels (Figure 2).

The signature polygons were initially determined based on the most up-to-date orthophotomaps from 2017–2020 with resolution of 0.25–0.5 m provided by GUGIK and verified by inspection in-situ. As a results of the works carried out in this part of the research, a set of polygons was created in the geodatabase developed for the purposes of the Geographic Information System, containing: 41 signatures for class 1, 42 signatures for class 2, and 41 signatures for class 3.

2.3.3. Preparation of spectral signatures database based on remote sensing data

For all the dates indicated in Table 1, 8 thematic maps were drawn, representing the values of VI (as indicated in Table 3). Conversion of S-2 images to maps was performed using the methods described in chapter 2.2.2. Descriptive
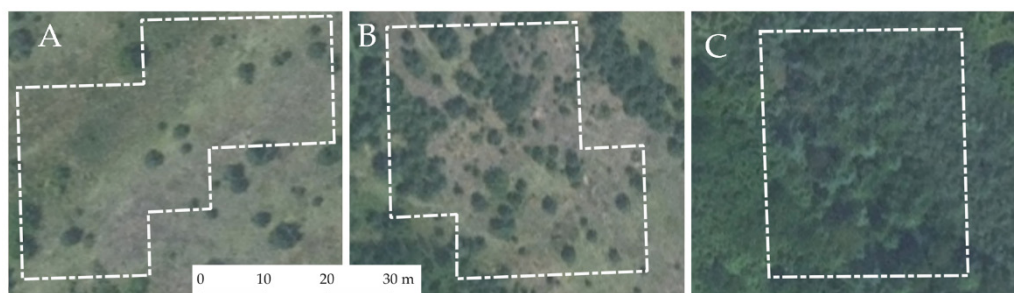

Figure 3. Example of polygons representing classes of natural succession: A – class 1; B – class 2; C – class 3

statistics were then calculated for each spectral signature. Since the sample of pixels within each polygon was not numerous (at least 9 to a dozen or so pixels), and the presence of objects from outside the class was allowed (see three bushes visible in Figure 2A) statistical distributions of index values do not meet the conditions of normal distribution. For this reason, the median and quartiles were adopted as statistical measures. The analysis was performed using the RStudio software (Hijmans, 2020). The direct result of this step was a table of spectral signature polygon attributes with class descriptive statistics.

2.3.4. Method for determining the best observation periods

In the next step of the analysis, it was examined whether statistically significant differences and dependencies between the values of individual vegetation indices could be identified for individual succession classes, and which stage of vegetation would potentially allow for separation of these classes in the process of index maps' classification – it should be noted here that demonstrating the possibility of class separation based on VI is a *sine qua non* condition for developing a classification model and thus validating the working hypothesis.

In order to recognize the differences in the distribution of VI values within the polygons of individual classes, these dependencies were visualized with box plots, which allowed for the initial recognition of dispersion and differences in the values of the median and quartiles for each date and class of succession. A complete picture of this analysis is included in Appendix 1 (Figure A 1-8).

Then, statistical inference was performed. The Shapiro-Wilk test confirmed the expected lack of normal distribution of individual groups, therefore, to assess the diversity of VI values in 3 succession classes, the nonparametric Kruskal-Wallis test was performed, which did not require the above assumption (Kruskal, 1952; Kruskal, Wallis, 1952). In order to find out, which groups (succession classes) differed significantly, the method of multiple comparisons was applied for all dates of satellite images' acquisition. As a result of the statistical analysis, a set of measures was obtained to determine the significance of the difference in the spectral reflectance between the succession classes in all the available periods indicated in Table 1.

2.3.5. Classification model

The construction of the model constitutes the main utilitarian goal of this work. The model was assumed to serve as a functional tool for assessing the degree of natural succession on abandoned land in Poland. The following criteria were adopted in the algorithmization process:

For the classification process, satellite images from the most appropriate periods will be selected – i.e. those, when the best separation of spectral signatures is observed (see 2.3.2).

The classification can be based on a combination of periods and vegetation indices – namely, determination of belonging to a classified pixel may depend on the results obtained in different periods. This assumption ensues mainly from the fact that the species identified as markers for given classes have certain spectral properties which are characteristic for them in different periods of vegetation, e.g. goldenrod, being such an indicator species for class 1, blooms at the turn of August and September, which is a characteristic feature of this plant allowing for separation of its site from other types of vegetation cover – especially trees and shrubs.

The model is to be based on a deterministic decision tree algorithm, using previous statistical analyses

The model is to be open to future modifications and extensions – therefore, algorithms and analytical tools were programmed in an open source environment.

The performance of the model will be verified by its validation using an independent sample of data (see 2.3.6).

2.3.6. Assessment of classification accuracy

In order to perform a quantitative analysis of the classification accuracy, the confusion matrix was used, the representations of which are visualized in Table 4, which allowed for the calculation of the classification evaluation metric (Foody, 2002; Hejmanowska, Wężyk, 2020).

Table 4. Error Matrix Example.

		Reference points i			
		Class 1	Class 2	Class 3	sum
Prediction points j	Class 1	n11	n21	n31	n1j sum (n11,n21,n31)
	Class 2	n12	n22	n32	n2j sum (n12,n22,n32)
	Class 3	n13	n23	n33	n3j sum (n13,n23,n33)
	sum	n1i	n2i	n3i	n

Overall Accuracy – OA – is the quotient of the sum of correctly classified points and the total number of points:

$$\mathbf{OA} = \frac{n11 + n22 + n33}{n}$$

Producer's accuracy" – PA – is expressed by the ratio of correctly classified points in a given class to the total number of points of this class in the reference data (example for class 1):

$$\mathbf{PA} = \frac{n11}{n1i}$$

User's accuracy – UA – is the ratio of points correctly classified in a class to the total number of points of this class in the prediction image (example for class 1):

$$UA = \frac{n11}{n1j}$$

Kappa coefficient – defines the total classification error and the degree of agreement between compared images. It takes the value of 0–1, where 1 means full agreement and 0 – agreement at the level that would occur for a random distribution of data.

3. RESULTS

3.1. Selection of dates and indices for the succession degree classification model

In line with the chosen methodology (sections 2.3.3 and 2.3.4), the pre-selection was conducted based on the analysis of the diversity of spectral signature distribution, visualized using the box plot method. When analyzing changes in the course of spectral reflection characteristics in time, four most convenient dates were indicated, in which the greatest separation of VI value distributions occurs. These are as follows: February 19 (winter); April 15 (spring); August 28 (summer); October 12 (autumn). The best results were obtained for the GNDVI index, where, in all the indicated periods, almost a complete separation was observed for the intervals (between the lower and upper quartile) in all three classes (Figure 4). In this respect, the GNDVI index clearly stood out among all the other indicators. However, the too short range of diversification of values both for classes in the studied periods and for their annual distribution may be problematic. Equally promising results for the whole vegetation season were obtained for NDVI, in case of which a greater diversification in amplitudes during the season was observed, yet for one period (August, 28) the upper quartile of the second class coincides with the lower quartile of the third class. One can also notice a weaker separation in the winter and spring seasons (in relation to GNDVI) – see Figure A1 vs. Figure A7.

In the case of other indicators, only the selected dates offer a possibility to distinguish between the succession classes spectrally. The NDVI, NDVIre2 and NDVIre3 indices are very similar in this regard; on June 14, the differences between all classes in terms of these three indicators were not statistically significant, while for June 9, the NDVI index separated only classes 1 and 3, and for NDVIre3 it was not possible to separate class 1 and 2. In general, the most favorable dates were in early spring and autumn. In the case of the NDVIre1 index, a complete separation of succession classes was possible only for three dates in early spring, however, on April 25 the quartile cutoffs did not coincide (Figure A1–A4). Also on this date, there is a clear class 3 separation observed for all NDVI derived indices. This is the moment when tree vegetation starts, while uncut, dry biomass of perennial plants (class 1) blocks the spectral reflection of young shoots. However, in the case of class 2, it is the moment of flowering for some shrubs, e.g. blackthorn (*Prunus spinosa* L.), which may cause lower values of the NDVI index.

In the case of SAVI and EVI indicators, the separation of the three classes was significantly impeded (Figure A5 and Figure A6). For SAVI, it was potentially possible only for the following dates: February 19, March 31, April 15, April 25, and for EVI only for February 19, March 31.
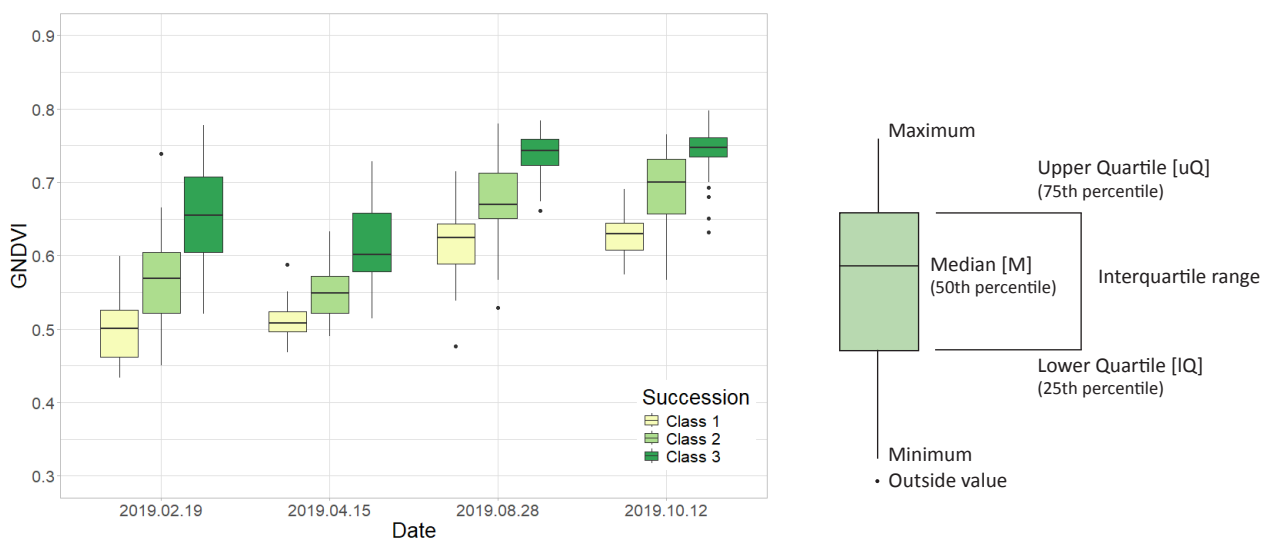

Figure 4. Distribution of GNDVI values for three succession classes on the following selected dates: 2019.02.19; 2019.04.15; 2019.08.28; 2019.10.12. The distribution for all examined dates is presented in Figure A7 (Appendix A).

The last indicator is NDRE using the near infrared bands and red edge. This is the only indicator for which the potential separation of classes is possible in summer and late spring, when the culmination of vegetation occurs. However, the high dispersion of its values can prove problematic in determining threshold values for the classification (Figure A8). Box plots for all the indices are listed in Appendix A (Figure A1– A8).

The results of the box plot analysis were confirmed with the Kruskal-Wallis ANOVA test, which in the case of the GNDVI index showed the significance of distribution separation in all three succession classes, for 12 out of 14 dates ($p < 0.000001$) and in case of NDVI for 11 out of 14 dates. To compare, the SAVI index allowed for performing classification only for four dates, and EVI only for two (Appendix A, Table A1).

3.2. Classificaton model

The classification model was programmed and run in the QGIS environment, which allowed for a direct access to the geodatabase (VI maps developed based on satellite images). The algorithms were based on the principles adopted in chapter 2.3.5 and on the preliminary results allowing for the selection of appropriate indicators (VI) and vegetation periods in which these indicators are the most diverse, thereby allowing for mapping the degree of natural succession within the analyzed agricultural plots. The final image of the model structure is presented in Figure 5a–d, which illustrates how the classification rules were applied to assign pixels to a given succession class in each of the four selected dates. Whereas Tables 5–8 summarize the values of median, lower quartile (lQ) and upper quar-

Table 5. Conditions for classification dated 2019.02.19.

| | **GNDVI** | | | **NDVI** | | | **NDRE** | | |
	Median	lQ	uQ	Median	lQ	uQ	Median	lQ	uQ
Class 1	0.5006	0.4622	0.5259	0.3270	0.3045	0.3728	0.2230	0.1920	0.2506
Class 2	0.5693	0.5210	0.6057	0.4378	0.3723	0.5143	0.2854	0.2127	0.3283
Class 3	0.6545	0.6043	0.7075	0.5251	0.4754	0.6924	0.3911	0.3113	0.4500

lQ – lower Quartile, uQ – upper Quartile

Table 6. Conditions for classification dated 2019.04.15.

| | **GNDVI** | | | **NDVIre1** | | | **NDVIre2** | | |
	Median	lQ	uQ	Median	lQ	uQ	Median	lQ	uQ
Class 1	0.5084	0.4966	0.5237	0.1533	0.1355	0.1789	0.3095	0.2810	0.3451
Class 2	0.5494	0.5215	0.5726	0.1985	0.1738	0.2311	0.3680	0.3214	0.4156
Class 3	0.6015	0.5782	0.6584	0.2756	0.2389	0.3412	0.4807	0.4194	0.5968

lQ – lower Quartile, uQ – upper Quartile

Table 7. Conditions for classification dated 2019.08.28.

| | **GNDVI** | | | **NDRE** | | |
	Median	lQ	uQ	Median	lQ	uQ
Class 1	0.6249	0.5865	0.6439	0.4369	0.3962	0.4639
Class 2	0.6692	0.6502	0.7144	0.4983	0.4491	0.5610
Class 3	0.7433	0.7231	0.7584	0.6021	0.5619	0.6248

lQ – lower Quartile, uQ – upper Quartile

Table 8. Conditions for classification dated 2019.10.12.

| | **GNDVI** | | | **NDVIre3** | | | **NDVI** | | |
	Median	lQ	uQ	Median	lQ	uQ	Median	lQ	uQ
Class 1	0.6301	0.6059	0.6450	0.6065	0.5666	0.6440	0.6301	0.5896	0.6685
Class 2	0.7005	0.6533	0.7320	0.7159	0.6506	0.7623	0.7310	0.6718	0.7781
Class 3	0.7471	0.7348	0.7613	0.7923	0.7666	0.8128	0.8052	0.7834	0.8227

lQ – lower Quartile, uQ – upper Quartile

Figure 5a. The Model for classifying the degree of natural succession on abandoned land – a set of algorithms for the date 2019.02.19 and the adopted variables determined based on the distributions of VI values (bottom). Box plot description see Figure 4.
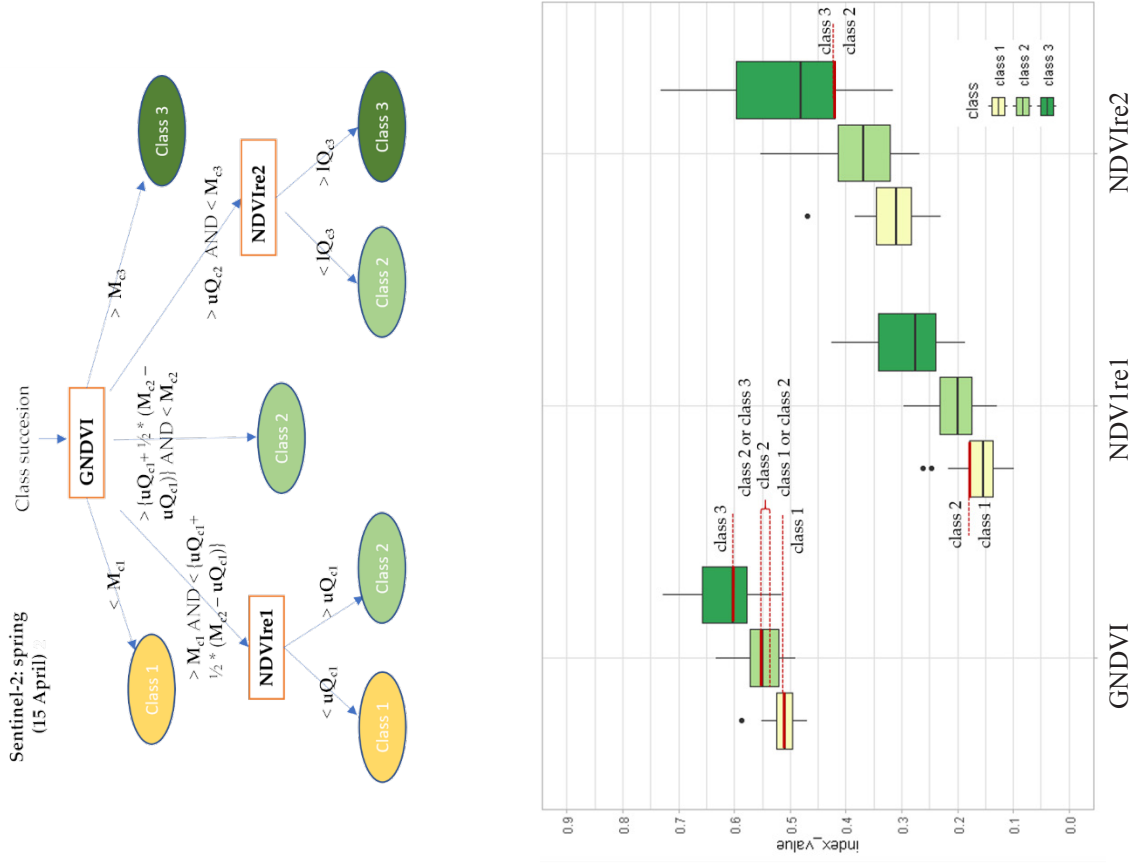
Figure 5b. The Model for classifying the degree of natural succession on abandoned land – a set of algorithms for the date 2019.04.15 and the adopted variables determined based on the distributions of VI values (bottom). Box plot description see Figure 4.
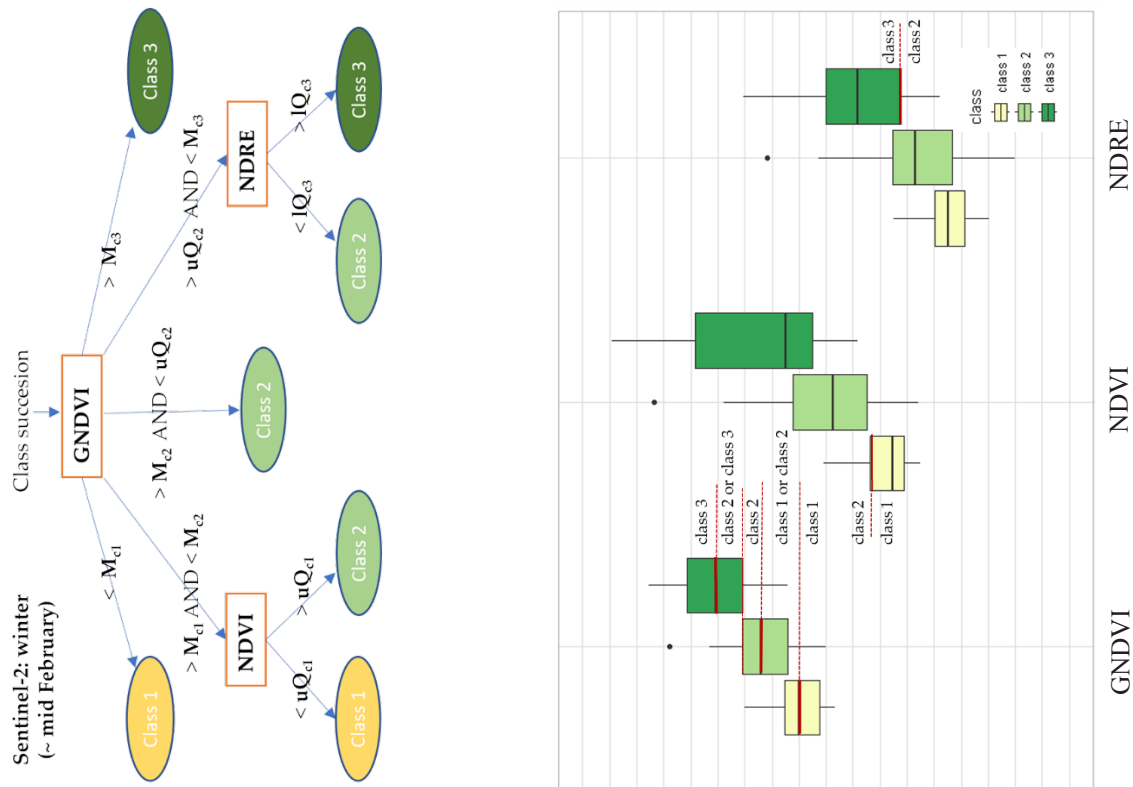
Figure 5d. The Model for classifying the degree of natural succession on abandoned land – a set of algorithms for the date 2019.10.12 and the adopted variables determined based on the distributions of VI values (bottom). Box plot description see Figure 4.

Figure 5c. The Model for classifying the degree of natural succession on abandoned land – a set of algorithms for the date 2019.08.28 and the adopted variables determined based on the distributions of VI values (bottom). Box plot description see Figure 4.
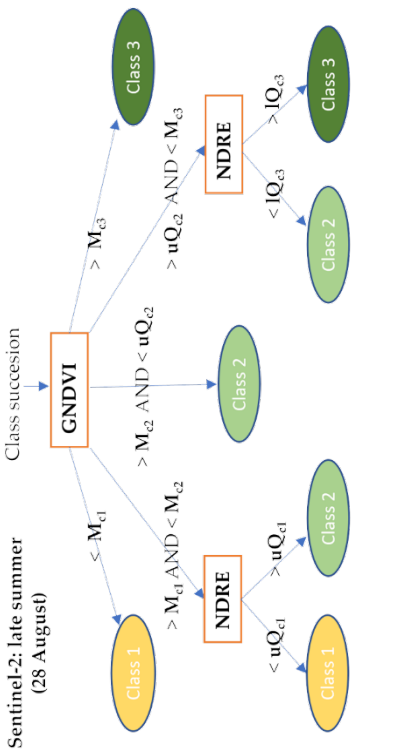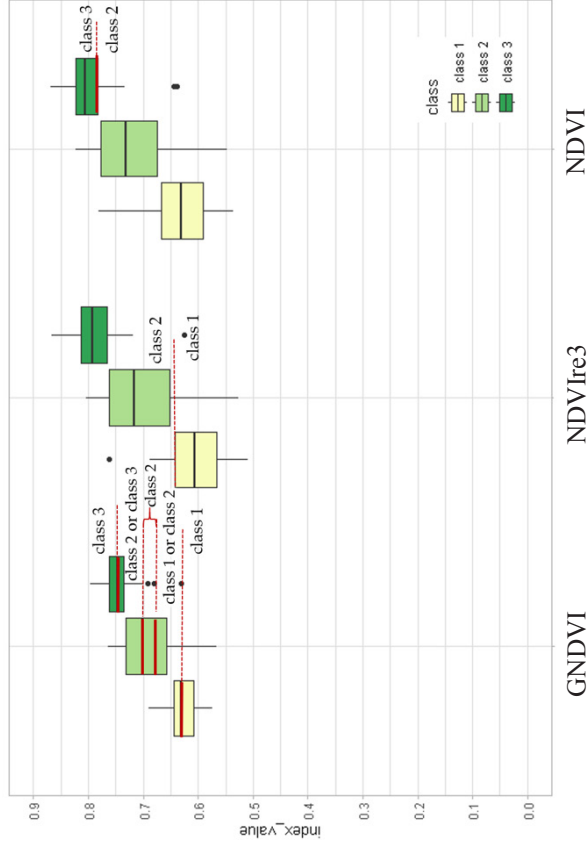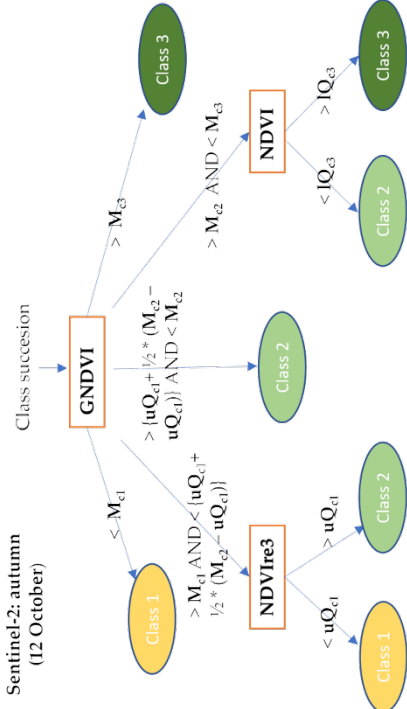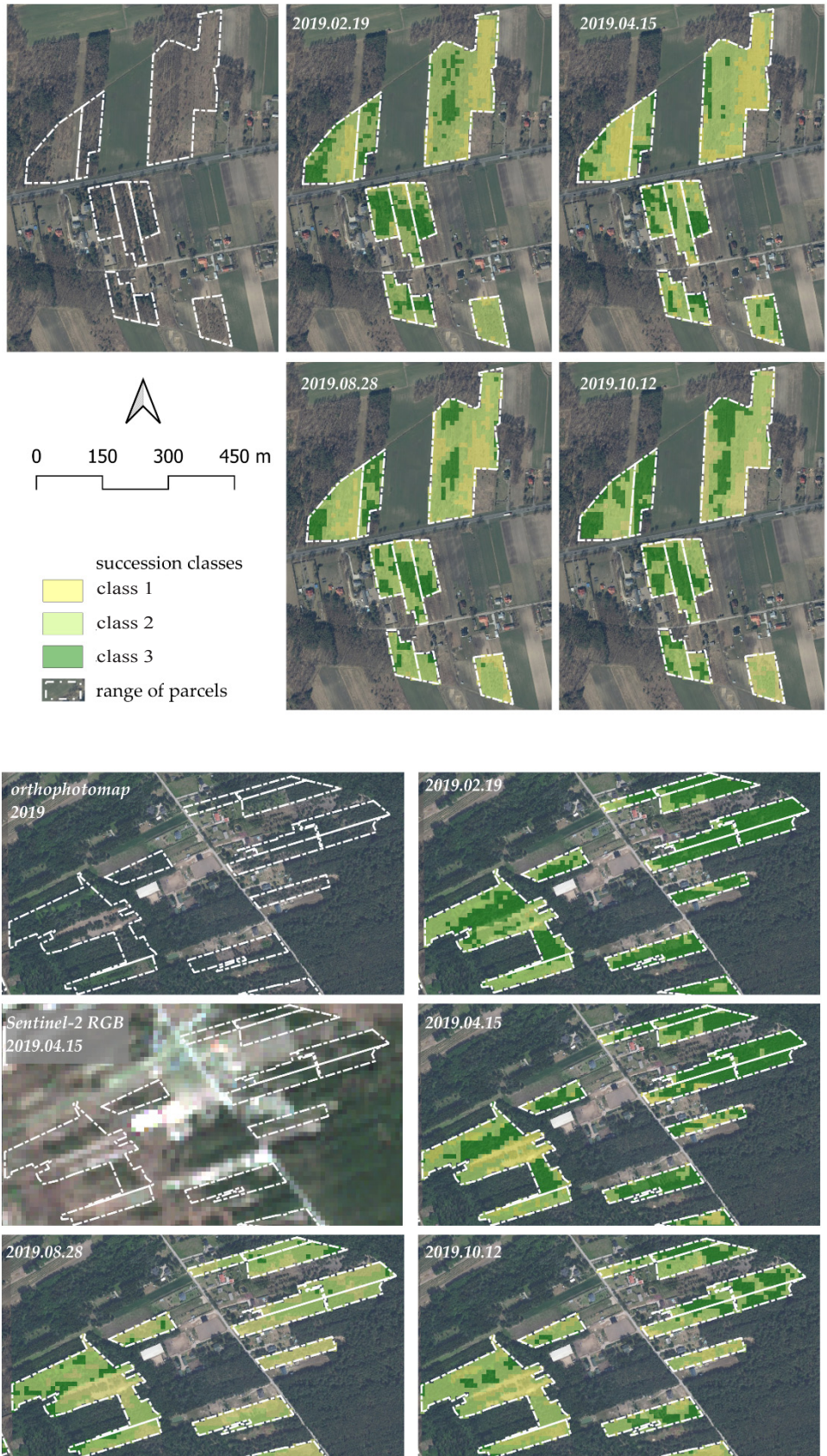
Figure 6. Examples of maps of natural succession degree classification, generated using the model – for the four selected dates.

tile (uQ) of each indicator (see box plot description in Figure 4).

For the first of the selected dates (February, 19), the advantage of good spectral separation illustrated by the GNDVI index for all classes of succession was used. In case of uncertainty between classes 1 and 2, the NDVI index was additionally used, and in the case of uncertainty between classes 2 and 3, the NDRE index was incorporated. In subsequent periods, the most appropriate indices to distinguish between classes 1 and 2, and 2 and 3 were respectively: NDVIre1 and NDVIre2 in the second period; NDRE in the third; and NDVIre3 and NDVI in the fourth. In this way, a deterministic model was built based on a combination of several vegetation indices, which at a given date are characterized by the best properties of registering reflected radiation for those spectral channels that best enable recognition of features characteristic for a given class of succession.

The direct effect of geoprocessing performed using the model was generation of four maps of succession classes at the assumed dates. An example of such maps in a raster format is presented in Figure 6. It should be noted that the adopted resolution of maps generated by the model corresponds to the highest spatial resolution of the Sentinel-2 images (10×10 m). Another relevant point is that the model allows for a difference in classification between individual dates – which is also visible in the presented example (Figure 6). As assumed at the beginning, the modelling accuracy for the indicated dates will only be estimated in the validation process.

3.3 Model validation result

In order to assess the accuracy of the results generated by the algorithms of the model, an independent validation set was randomly selected, consisting of 126 points, of which 36 points represented class 1 of succession, 49 class 2, and 41 class 3. Succession class attributes for each point were verified by eye observation. Validation was performed by direct comparison of the classification results with the situation observed on site. The accuracy assessment of each classification was performed using the QGIS SCP script (Congedo, 2021). Based on the calculated error matrix, which compares points with a field-verified succession degree attribute with the results obtained by classification performed using the developed model, the statistics of the overall model assessment are calculated: Total Accuracy (TA) and Kappa coefficient, as well as assessment of accuracy in classification to individual classes: User's accuracy (UA), Producer's accuracy (PA) – Table 9.

The analysis of the validation results presented in the table shows that the best overall results were ob-

2019.02.19	Class types determined from reference source					
Class types from classified map	Classes	1	2	3	Totals	User's accuracy
	1	34	10	0	44	**77.2**
	2	2	32	13	47	**68.1**
	3	0	7	28	35	**80.0**
	Totals	36	49	41	126	Total accuracy
Producer's Accuracy		**94.4**	**65.3**	**68.3**		**74.6**
Kappa						0.62
2019.04.15	Class types determined from reference source					
Class types from classified map	Classes	1	2	3	Totals	User's accuracy
	1	31	11	1	43	**72.1**
	2	5	30	11	46	**65.2**
	3	0	8	29	37	**78.4**
	Totals	36	49	41	126	Total accuracy
Producer's Accuracy		**86.1**	**61.2**	**70.7**		**71.4**
Kappa						0.60
2019.08.28	Class types determined from reference source					
Class types from classified map	Classes	1	2	3	Totals	User's accuracy
	1	28	4	3	35	**80.0**
	2	8	28	6	42	**66.7**
	3	0	17	32	49	**65.3**
	Totals	36	49	41	126	Total accuracy
Producer's Accuracy		**77.8**	**57.1**	**78.0**		**69.8**
Kappa						0.56
2019.10.12	Class types determined from reference source					
Class types from classified map	Classes	1	2	3	Totals	User's accuracy
	1	29	7	0	36	**80.5**
	2	7	37	14	58	**63.8**
	3	0	5	27	32	**84.4**
	Totals	36	49	41	126	Total accuracy
Producer's Accuracy		**80.6**	**75.6**	**65.9**		**73.8**
Kappa						0.80

tained for the winter period (2019.02.19), in which the TA index achieved the highest value (74.6) accompanied by an equally high value of Kappa (0.62). A similar result was obtained for the autumn period, where TA value is slightly lower (73.8), but Kappa value is the highest of all the modelled periods (0.8). The worst overall results were obtained for the summer period (2019.08.28), in which the lowest values were recorded for both TA (69.8) and Kappa (0.56).

When analyzing the possibility of separating individual classes, it should be noted that the use of the model for classifying satellite images in winter may give the best results for separating the first succession class. In this instance, 34 out of 36 samples were classified correctly (PA = 94.4). Class 3 (woody vegetation), on the other hand, was best visible in summer (PA = 78.0). Shrubs (class 2) were best identified in autumn (PA = 75.6).

An alternative method to indicate the modelled result best corresponding to the real situation is to assess the classification error for other classes in relation to the class under consideration (user's accuracy). In such case, the best results were obtained for separation of class 3 in autumn (UA = 84.4). However, when using this indicator, one should pay attention to PA, which in this case is very unfavorable (65.9) – this proves that this type of land cover is classified incorrectly as shrubs (14 cases out of 41).

4. DISCUSSION

4.1. Model accuraccy vs current needs

According to research conducted by Pudełko et al. (2018), currently in Poland over 2.7 million ha of agricultural land is not declared by farmers as the area under agricultural activity. This means that these areas have been set aside or transformed for other, non-agricultural needs without being reported to the land records. Another finding resulting from the studies is that 2.03 million ha constitute agricultural plots with an area of > 0.3 ha, where effective agricultural production can take place. On a national scale, this is a considerably large area – approx. 14% of the total area of agricultural land. The biggest paradox of this situation is that, so far, these areas have not been subject to any assessment. Such situation results from the methodology adopted by the Central Statistical Office, institution responsible for statistics and reporting of agricultural production, which in the case of abandoned land is not carried out (*The Agricultural Census 2020*, n.d.). Also, ARMA, which is the government agency responsible for the implementation of the CAP, does not have a registry of abandoned land – because there are no subsidies for this type of land. In 2004, when Poland became one of the EU countries, it was assumed that the problem of land abandonment would be solved by EU subsidies and farmers would restore these areas for agriculture. Alas, it did not happen.

The above-described situation has resulted in a constantly growing number of fallow lands. There is no data on their current condition, and no programs supporting any restoration of these areas for active use or systemic conversion to the so-called "environmental areas" subject to legal tools of nature protection, where habitats of natural and valuable vegetation for local ecosystems would be restored (Bell et al., 2020; Queiroz et al., 2014; Szirmai et al., 2022). However, due to the size of the discussed area, the investment potential of these lands is constantly growing. Future changes in landuse must, however, take into account the current state of abandoned land, which is most affected by the degree of natural succession. The presence of trees or bushes can be at the same time considered as an obstacle or, on the contrary, as a factor favouring the decision to liquidate fallow. An example of such may be the possibility of harvesting biomass in the process of removing self-seeding plants, especially when the succession is defined as class 3 according to classification described in this work (trees). On the market, there can already be found companies offering such services – but the plot must meet the criteria for the suitable amount of biomass (Stolarski et al., 2021, 2022).

Another example is the possibility of restoring abandoned land to agricultural production using the farmer's equipment and efforts – for this scenario, the preferred, and sometimes the only possible form of land cover is a complete lack of trees and bushes – i.e. class 1 as described in this work. Another aspect crucial for the possibility of implementing a policy of effective management of abandoned land is learning about its regionalization. As it has already been proved in the cited work (Pudełko et al., 2018), abandoned land is subject to regionalization both in terms of the area and shape of agricultural plots, as well as the general percentage of abandoned area in the region (Krysiak, 2011).

The above-characterized situation of recognizing the fallowing status indicates the need to carry out at least a general recognition of the degree of natural succession of abandoned land throughout the country as well as its regionalization.

4.2. Possibilities of increasing the assessment accuracy of abandoned land

Examples of spatial differentiation of natural succession within plots (visible e.g. in Figure 3) prove that resolution has a large impact on the definition of spectral signatures used in the model. When using polygons to test spectral characteristics, one can find it difficult to identify a representative area that fully meets the definition of a given class. For instance, in Figure 3A we can see the presence of bushes, and in Figure 3B there is a different density in the bushes. Theoretically, better classification results could be obtained by using image data with better spatial resolution, e.g. aerial orthophotomaps or VHR satellite images. Such accuracy allows for direct differentiation and separation of objects (trees, shrubs, infrastructure) and for better characteristics of these objects (e.g. distinguishing between coniferous and deciduous trees, assessment of biomass resources).

Other significant factors, in addition to spatial resolution, are: the ability to obtain data regardless of weather conditions and using subsequent spectral ranges. Both these factors are crucial in building the model's algorithm. In case of the former, the results clearly indicate the impact of the proper selection of the observation period. For images in the visible band, there may be great difficulties in obtaining data related to cloudiness or the presence of cloud shadows (Aybar et al., 2022). This problem can be eliminated or reduced by incorporating images from other satellites or by using radar images (Bucha et al., 2021;

Goga et al., 2019; Suziedelyte Visockiene et al., 2019). Currently, there are a number of national publications on the identification of unused agricultural land as well as detailed recognition and assessment of vegetation formation (Grabska-Szwagrzyk et al., 2024; Hawryło et al., 2018; Wakulińska, Marcinkowska-Ochtyra, 2020). However, there is a gap in knowledge about the possibilities of using Sentinel-2 images for a detailed assessment of the degree of advancement of natural succession. The classes of natural succession distinguished for the purposes of this study are characterized by great diversity, both in terms of species composition, degree of advancement and density. In this case, the dispersion and fragmentation of cadastral plots is also problematic, which is characteristic of the selected study region. The above-mentioned factors therefore pose a great challenge in terms of the selection of appropriate classification methods, dates of image acquisition and the use of appropriate vegetation indices. One of the publications in which 2 classes of succession were distinguished due to the height, density and maturity of succession, the shrub class and the forest class (Bucha et al., 2021). The authors in Slovakia used Sentinel-1 and Sentinel-2 images for a model for estimating biomass from unused agricultural land. correspond to the highest resolution of Sentinel-2 (10–20 m).

Increasing the accuracy of the abandoned land assessment model by supplementing the algorithm with successive indexes based on other spectral ranges seems to be of little importance. Hence, it is difficult to expect an improvement in accuracy by introducing mid-infrared ranges into the model (Morell-Monzó et al., 2020; Suziedelyte Visockiene et al., 2019; Szatmári et al., 2018; Tumelienė et al., 2021). A more effective solution may be the use of thermal images. However, the resolution of those images would have to correspond to the highest resolution of Sentinel-2 (10–20m).

5. CONCLUSIONS

The deterministic model of natural succession assessment presented in the paper for four dates of satellite image acquisition can be an effective tool for assessing the three adopted classes of natural succession. The validation results of the model proposed in this paper confirm the possibility of using this tool to conduct such kind of research. In this case, the main advantages of the model are as follows:

The use of imaging data (Sentinel-2) available for the entire country, with a high probability of obtaining materials within the indicated optimal periods

Spatial resolution of data which enables remote sensing of land cover diversification within agricultural parcels

The open code of the model algorithm that can be refined and supplemented with other data sources as needed

The validation results confirm also the sufficient effectiveness of the proposed method. Recognition of the

lack of advanced natural succession in the case of > 94.4% of plots is sufficient for developing regional strategies of restoration of abandoned land to agricultural production, without taking into account advanced financial outlays for the removal of self-seeding plants. In addition, the classification of high succession at the level of 78% enables harvesting of biomass in the process of landuse conversion – e.g. for purposes related to bioeconomy (Matyka, Radzikowski, 2020; Stolarski et al., 2020; Von Cossel et al., 2019).

The main indicator on which the natural succession assessment model was based is GNDVI. Its properties allowed for the best differentiation between the three adopted classes of natural succession. NDVI, NDRE, NDVIre1, NDVIre2, NDVIre3 were used as auxiliary indicators, which, as shown in the studies, can improve the accuracy of classification at a higher uncertainty threshold in the case of a weaker separation of classes by the GNDVI index.

The approach used in the development (modelling) of data may provide an indication of the method of changing the management of long-term fallow lands, which may be used in practice in spatial planning and creating the state's agricultural policy.

5.1. Further research directions

Guided by the possibilities indicated in the above section, future research conducted by the team of authors will focus on the following aspects:

- Assessing whether increasing the resolution of image data may affect modelling results. For this purpose, available aerial orthophotomaps (RGB) and indexes based on combinations of radiation reflection in the blue, green and red range will be used. The research will analyse the possibility of using this datasource only or in combination with Sentinel-2 imagery.
- Introducing Sentinel-1 radar data to the model, which will eliminate the problems caused by cloud cover.

Recognizing the possibility of assessing biomass resources that can be obtained by elimination of natural succession on abandoned land.

REFERENCES

Abdi A.M., 2020. Land cover and land use classification performance of machine learning algorithms in a boreal landscape using Sentinel-2 data. GIScience & Remote Sensing, 57(1), Article 1, https://doi.org/10.1080/15481603.2019.1650447.

Alonso F., Martínez-Hernández C., Díaz A., Cánovas-García F., Castillo F., 2015. Main Environmental Features Leading to Recent Land Abandonment in Murcia Region (Southeast Spain). Land Degradation & Development, 27, https://doi.org/10.1002/ldr.2447.

Anguiano E., Bamps C., Terres J., Pointereau P., Coulon F., Girard P., Lambotte M., Stuczynski T., Sanchez O.V.,

Del R.A., 2008. Analysis of Farmland Abandonment and the Extent and Location of Agricultural Areas that are Actually Abandoned or are in Risk to be Abandoned. JRC Publications Repository, https://publications.jrc.ec.europa.eu/repository/handle/JRC46185.

Aybar C., Ysuhuaylas L., Loja J., Gonzales K., Herrera F., Bautista L., Yali R., Flores A., Diaz L., Cuenca N., Espinoza W., Prudencio F., Llactayo V., Montero D., Sudmanns M., Tiede D., Mateo-García G., Gómez-Chova L., 2022. CloudSEN12, a global dataset for semantic understanding of cloud and cloud shadow in Sentinel-2. Scientific Data, 9(1), 782, https://doi.org/10.1038/s41597-022-01878-2.

Barnes E., Clarke T.R., Richards S.E., Colaizzi P., Haberland J., Kostrzewski M., Waller P., Choi C., Riley E., Thompson T.L., 2000. Coincident detection of crop water stress, nitrogen status, and canopy density using ground based multispectral data. 15 pp. Proceedings of the Fifth International Conference on Precision Agriculture.

Bell S.M., Barriocanal C., Terrer C., Rosell-Melé A., 2020. Management opportunities for soil carbon sequestration following agricultural land abandonment. Environmental Science & Policy, 108: 104-111, https://doi.org/10.1016/j.envsci.2020.03.018.

Bucha T., Papčo J., Sačkov I., Pajtík J., Sedliak M., Barka I., Feranec J., 2021. Woody Above-Ground Biomass Estimation on Abandoned Agriculture Land Using Sentinel-1 and Sentinel-2 Data. Remote Sensing, 13(13), Article 13, https://doi.org/10.3390/rs13132488.

CAP 2023-27–European Commission. https://agriculture.ec.europa.eu/common-agricultural-policy/cap-overview/cap-2023-27_en (accessed 2024, September 13).

Collier M., 2018. Farmland abandonment in Europe: An overview of drivers, consequences and assessment of the sustainability implications. https://doi.org/10.1139/er-2018-0001#.W3HYqi3MyrP.

Congedo L., 2021. Semi-Automatic Classification Plugin: A Python tool for the download and processing of remote sensing images in QGIS. The Journal of Open Source Software, 6, 3172, https://doi.org/10.21105/joss.03172.

Dara A., Baumann M., Kuemmerle T., Pflugmacher D., Rabe A., Griffiths P., Hölzel N., Kamp J., Freitag M., Hostert P., 2018. Mapping the timing of cropland abandonment and recultivation in northern Kazakhstan using annual Landsat time series. Remote Sensing of Environment, 213: 49-60, https://doi.org/10.1016/j.rse.2018.05.005.

Directive–2018/2001–EN - EUR-Lex. (n.d.). https://eur-lex.europa.eu/eli/dir/2018/2001/oj (accessed 20 September 2024.

Eco-schemes–European Commission. (2024, February 13). https://agriculture.ec.europa.eu/common-agricultural-policy/income-support/eco-schemes_en.

Elbersen B.S., Beaufoy G., Jones G., Noij I., Breman B.C., Hazeu G.W., 2014. Aspects of data on diverse relationships between agriculture and the environment.

Estel S., Kuemmerle T., Alcántara C., Levers C., Prishchepov A., Hostert P., 2015. Mapping farmland abandonment and recultivation across Europe using MODIS NDVI time series. Remote Sensing of Environment, 163: 312-325, https://doi.org/10.1016/j.rse.2015.03.028.

Falińska K., 1997. Ekologia roślin. Wydawnictwo Naukowe PWN.

Foody G.M., 2002. Status of land cover classification accuracy assessment. Remote Sensing of Environment, 80(1): 185-201, https://doi.org/10.1016/S0034-4257(01)00295-4.

Geoportal.gov.pl. (n.d.). https://mapy.geoportal.gov.pl/imap/Imgp_2.html?gpmap=gp0 (accessed 20 September 2024).

Gitelson A.A., Merzlyak M.N., 1998. Remote sensing of chlorophyll concentration in higher plant leaves. Advances in Space Research, 22(5), Article 5, https://doi.org/10.1016/S0273-1177(97)01133-2.

Goga T., Feranec J., Bucha T., Rusnák M., Sačkov I., Barka I., Kopecká M., Papčo J., Oťaheľ J., Szatmári D., Pazúr R., Sedliak M., Pajtík J., Vladovič J., 2019. A Review of the Application of Remote Sensing Data for Abandoned Agricultural Land Identification with Focus on Central and Eastern Europe. Remote Sensing, 11(23), Article 23, https://doi.org/10.3390/rs11232759.

Grabska-Szwagrzyk E., Tiede D., Sudmanns M., Kozak J., 2024. Map of forest tree species for Poland based on Sentinel-2 data. Earth System Science Data, 16(6): 2877-2891, https://doi.org/10.5194/essd-16-2877-2024.

Grădinaru S.R., Kienast F., Psomas A., 2019. Using multi-seasonal Landsat imagery for rapid identification of abandoned land in areas affected by urban sprawl. Ecological Indicators, 96Ł 79+86. https://doi.org/10.1016/j.ecolind.2017.06.022

Gutman G., Radeloff V. C. (Eds.)., 2017. Land-Cover and Land-Use Changes in Eastern Europe after the Collapse of the Soviet Union in 1991. Springer.

Hansen P.M., Schjoerring J.K., 2003. Reflectance measurement of canopy biomass and nitrogen status in wheat crops using normalized difference vegetation indices and partial least squares regression. Remote Sensing of Environment, 86(4): 542–553, https://doi.org/10.1016/S0034-4257(03)00131-7.

Hawryło P., Bednarz B., Wężyk P., Szostak M., 2018. Estimating defoliation of Scots pine stands using machine learning methods and vegetation indices of Sentinel-2. European Journal of Remote Sensing, 51(1), Article 1, https://doi.org/10.1080/22797254.2017.1417745.

Hejmanowska B., Wężyk P. (Eds.), 2020. Dane satelitarne dla administracji publicznej. e-ISBN: 978-83-945436-3-1, https://polsa.gov.pl/wp-content/themes/polsa/files/Podrecznik.pdf

Herrmann I., Pimstein A., Karnieli A., Cohen Y., Alchanatis V., Bonfil D.J., 2011. LAI assessment of wheat and potato crops by VENμS and Sentinel-2 bands. Remote Sensing of Environment, 115(8): 2141-2151, https://doi.org/10.1016/j.rse.2011.04.018.

Hijmans R.J., 2020. terra: Spatial Data Analysis. R apckage version 1.7-78. https://doi.org/10.32614/CRAN.package.terra.

Huete A., Didan K., Miura T., Rodriguez E.P., Gao X., Ferreira L.G., 2002. Overview of the radiometric and biophysical performance of the MODIS vegetation indices. Remote Sensing of Environment, 83(1–2), Article 1–2, https://doi.org/10.1016/S0034-4257(02)00096-2.

Huete A.R., 1988. A soil-adjusted vegetation index (SAVI). Remote Sensing of Environment, 25(3), Article 3, https://doi.org/10.1016/0034-4257(88)90106-X.

IDB - Index DataBase. (n.d.). https://www.indexdatabase.de/ (accessed 21 August 2024).

Jabs-Sobocińska Z., Affek A.N., Ewiak I., Nita M.D., 2021. Mapping Mature Post-Agricultural Forests in the Polish

Eastern Carpathians with Archival Remote Sensing Data. *Remote Sensing*, *13*(10), Article 10, https://doi.org/10.3390/rs13102018.

Janus J., Bożek P., 2019. Land abandonment in Poland after the collapse of socialism: Over a quarter of a century of increasing tree cover on agricultural land. Ecological Engineering, 138: 106-117, https://doi.org/10.1016/j.ecoleng.2019.06.017.

Kolecka N., 2018. Height of Successional Vegetation Indicates Moment of Agricultural Land Abandonment. Remote Sensing, 10(10), Article 10, https://doi.org/10.3390/rs10101568.

Kolecka N., 2021. Greening trends and their relationship with agricultural land abandonment across Poland. Remote Sensing of Environment, 257, 112340, https://doi.org/10.1016/j.rse.2021.112340.

Kolecka N., Kozak J., 2019. Wall-to-Wall Parcel-Level Mapping of Agricultural Land Abandonment in the Polish Carpathians. Land, 8(9), Article 9, https://doi.org/10.3390/land8090129.

Kolecka N., Kozak J., Kaim D., Dobosz M., Ostafin K., Ostapowicz K., Wężyk P., Price B., 2017. Understanding farmland abandonment in the Polish Carpathians. Applied Geography, 88: 62–72, https://doi.org/10.1016/j.apgeog.2017.09.002.

Kozak M., Pudełko R., 2021. Impact assessment of the long-term fallowed land on agricultural soils and the possibility of their return to agriculture. Agriculture, 11(2), Article 2, https://doi.org/10.3390/agriculture11020148.

Kruskal W.H., 1952. A Nonparametric test for the Several Sample Problem. The Annals of Mathematical Statistics, 23(4): 525-540, https://doi.org/10.1214/aoms/1177729332.

Kruskal W.H., Wallis W.A., 1952. Use of Ranks in One-Criterion Variance Analysis. Journal of the American Statistical Association, 47(260): 583-621, https://doi.org/10.1080/01621459.1952.10483441.

Krysiak S., 2011. Fallow lands in the landscapes of central Poland–Spatial, typological and ecological aspects (6–1). XXXI(6–1), Article 6–1.

Lasanta T., Nadal-Romero E., Arnáez J., 2015. Managing abandoned farmland to control the impact of re-vegetation on the environment. The state of the art in Europe. Environmental Science & Policy, 52: 99-109, https://doi.org/10.1016/j.envsci.2015.05.012

Macintyre P., van Niekerk A., Mucina L., 2020. Efficacy of multi-season Sentinel-2 imagery for compositional vegetation classification. International Journal of Applied Earth Observation and Geoinformation, 85, 101980, https://doi.org/10.1016/j.jag.2019.101980.

Matyka M., Radzikowski P., 2020. Productivity and Biometric Characteristics of 11 Varieties of Willow Cultivated on Marginal Soil. Agriculture, 10(12), Article 12. https://doi.org/10.3390/agriculture10120616.

Morell-Monzó S., Estornell J., Sebastiá-Frasquet M.-T., 2020. Comparison of Sentinel-2 and High-Resolution Imagery for Mapping Land Abandonment in Fragmented Areas. Remote Sensing, 12(12), Article 12, https://doi.org/10.3390/rs12122062.

Pudełko R., Kozak M., Jędrejek A., Gałczyńska M., Pomianek B., 2018. Regionalisation of unutilised agricultural area in Poland. Polish Journal of Soil Science, 51(1), Article 1, https://doi.org/10.17951/pjss.2018.51.1.119.

Queiroz C., Beilin R., Folke C., Lindborg R., 2014. Farmland abandonment: Threat or opportunity for biodiversity conservation? A global review. Frontiers in Ecology and the Environment, 12(5): 288-296, https://doi.org/10.1890/120348.

Ranghetti L., Boschetti M., Nutini F., Busetto L., 2020. "sen2r": An R toolbox for automatically downloading and preprocessing Sentinel-2 satellite data. Computers & Geosciences, 139, 104473, https://doi.org/10.1016/j.cageo.2020.104473.

Rouse J.W., Haas R.H., Schell J.A., Deering D.W., 1974. Monitoring vegetation systems in the Great Plains with ERTS. Paper A 20, https://ntrs.nasa.gov/citations/19740022614.

Sentinel-2. (n.d.). https://sentiwiki.copernicus.eu/web/sentinel-2 (accessed 20 September 2024).

Shahbandeh M., Kaim D., Kozak J., 2022. The Substantial Increase of Forest Cover in Central Poland Following Extensive Land Abandonment: Szydłowiec County Case Study. Remote Sensing, 14(16), Article 16, https://doi.org/10.3390/rs14163852.

Sosnowska A.J., 2019. Changes of vegetation effects in soil properties in the post-agriculture landscapes (south-eastern Poland). Miscellanea Geographica, 23(1), Article 1, https://doi.org/10.2478/mgrsd-2018-0032.

Stolarski M.J., Dudziec P., Olba-Zięty E., Stachowicz P., Krzyżaniak M., 2022. Forest Dendromass as Energy Feedstock: Diversity of Properties and Composition Depending on Systematic Genus and Organ. Energies, 15(4), Article 4, https://doi.org/10.3390/en15041442.

Stolarski M.J., Rosenqvist H., Krzyżaniak M., Szczukowski S., Tworkowski J., Gołaszewski J., Olba-Zięty E., 2015. Economic comparison of growing different willow cultivars. Biomass and Bioenergy, 81: 210-215, https://doi.org/10.1016/j.biombioe.2015.07.002.

Stolarski M.J., Stachowicz P., Sieniawski W., Krzyżaniak M., Olba-Zięty E., 2021. Quality and Delivery Costs of Wood Chips by Railway vs. Road Transport. Energies, 14(21), Article 21, https://doi.org/10.3390/en14216877.

Stolarski M.J., Szczukowski S., Krzyżaniak M., Tworkowski J., 2020. Energy Value of Yield and Biomass Quality in a 7-Year Rotation of Willow Cultivated on Marginal Soil. Energies, 13(9), Article 9, https://doi.org/10.3390/en13092144.

Stolarski M., Niksa D., Krzyżaniak M., Tworkowski J., Szczukowski S., 2019. Willow productivity from small- and large-scale experimental plantations in Poland from 2000 to 2017. Renewable and Sustainable Energy Reviews, 101: 461-475, https://doi.org/10.1016/j.rser.2018.11.034.

Stuczynski T., Siebielec G., Korzeniowska-Puculek R., Koza P., Pudelko R., Lopatka A., Kowalik M., 2009. Geographical location and key sensitivity issues of post-industrial regions in Europe. Environmental Monitoring and Assessment, 151(1): 77–91, https://doi.org/10.1007/s10661-008-0251-4.

Study of conditions and directions of spatial development. (n.d.). Pulawy commune. https://gminapulawy.pl/studium-uwarunkowan-i-kierunkow-zagospodarowania-przestrzennego/ (accessed 20 September 2024).

Suziedelyte Visockiene J., Tumeliene E., Maliene V., 2019. Analysis and identification of abandoned agricultural land using remote sensing methodology. Land Use Policy, 82: 709-715, https://doi.org/10.1016/j.landusepol.2019.01.013.

Szatmári D., Kopecka M., Feranec J., Goga T., 2018. Abandoned agricultural land mapping using Sentinel-2A data.

Szirmai O., Saláta D., Benedek L.K., Czóbel S., 2022. Investigation of the Secondary Succession of Abandoned Areas

from Different Cultivation in the Pannonian Biogeographic Region. Agronomy, 12(4), Article 4, https://doi.org/10.3390/agronomy12040773.

Szostak M., Hawryło P., Piela D., 2018. Using of Sentinel-2 images for automation of the forest succession detection. European Journal of Remote Sensing, 51(1), Article 1, https://doi.org/10.1080/22797254.2017.1412272.

Szostak M., Wężyk P., Hawryło P., Puchała M., 2016. Monitoring the Secondary Forest Succession and Land Cover/Use Changes of the Błędów Desert (Poland) Using Geospatial Analyses. Quaestiones Geographicae, 35(3): 1-13, https://doi.org/10.1515/quageo-2016-0022.

The Agricultural Census 2020. (n.d.). https://bdl.stat.gov.pl/bdl/dane/podgrup/temat (accessed 26 September 2024).

Thompson C.N., Guo W., Sharma B., Ritchie G.L., 2019. Using Normalized Difference Red Edge Index to Assess Maturity in Cotton. Crop Science, 59(5): 2167–2177, https://doi.org/10.2135/cropsci2019.04.0227.

Toure S.I., Stow D.A., Shih H., Weeks J., Lopez-Carr D., 2018. Land cover and land use change analysis using multi-spatial resolution data and object-based image analysis. Remote Sensing of Environment, 210: 259-268, https://doi.org/10.1016/j.rse.2018.03.023.

Trystuła A., Konieczna J., 2008. Land parcel management system in Poland and a case study of EU member states. Geodetski Vestnik, 62(04): 630–640, https://doi.org/10.15292/geodetski-vestnik.2018.04.630-640.

Tumelienė E., Visockienė J.S., Malienė V., 2021. The Influence of Seasonality on the Multi-Spectral Image Segmentation for Identification of Abandoned Land. Sustainability, 13(12), Article 12, https://doi.org/10.3390/su13126941.

Von Cossel M., Lewandowski I., Elbersen B., Staritsky I., Van Eupen M., Iqbal Y., Mantel S., Scordia D., Testa G., Cosentino S.L., Maliarenko O., Eleftheriadis I., Zanetti F., Monti A., Lazdina D., Neimane S., Lamy I., Ciadamidaro L., Sanz M., Alexopoulou E., 2019. Marginal Agricultural Land Low-Input Systems for Biomass Production. Energies, 12(16), Article 16, https://doi.org/10.3390/en12163123.

Wakulińska M., Marcinkowska-Ochtyra A., 2020. Multi-Temporal Sentinel-2 Data in Classification of Mountain Vegetation. Remote Sensing, 12(17), Article 17, https://doi.org/10.3390/rs12172696.

Yin H., Prishchepov A.V., Kuemmerle T., Bleyhl B., Buchner J., Radeloff V.C., 2018. Mapping agricultural land abandonment from spatial and temporal segmentation of Landsat time series. Remote Sensing of Environment, 210: 12–24, https://doi.org/10.1016/j.rse.2018.02.050.

Yusoff N.M., Muharam F.M., Takeuchi W., Darmawan S., Abd Razak M.H., 2017. Phenology and classification of abandoned agricultural land based on ALOS-1 and 2 PAL-SAR multi-temporal measurements. International Journal of Digital Earth, 10(2): 155–174, https://doi.org/10.1080/17538947.2016.1216615.

Zhu X., Xiao G., Zhang D., Guo L., 2021. Mapping abandoned farmland in China using time series MODIS NDVI. Science of The Total Environment, 755, 142651, https://doi.org/10.1016/j.scitotenv.2020.142651.

Author	ORCID
Małgorzata Kozak	0000-0003-4595-2825
Anna Jędrejek	0000-0001-8541-4410
Rafał Pudełko	0000-0002-6373-6272

Appendix A

Table A1. Multiple Comparsions p values of the tested vegetation indices based on the post-hoc (Dunn Bonferroni) at 95% level of significance (the green cells indicate statistically significant differences between classes of succession). cl. – succession classes; date – dates Sentinel 2 acquisitions.

date	NDVI				NDVIre1				NDVIre2			
2019_02_19	**p<0.000001**	cl. 1	cl. 2	cl. 3	**p<0.000001**	cl. 1	cl. 2	cl. 3	**p<0.000001**	cl. 1	cl. 2	cl. 3
	cl. 1		🟩	🟩	cl. 1		🟩	🟩	cl. 1		🟩	🟩
	cl. 2	🟩		🟩	cl. 2	🟩		🟩	cl. 2	🟩		🟩
	cl. 3	🟩	🟩		cl. 3	🟩	🟩		cl. 3	🟩	🟩	
2019_03_31	**p<0.000001**	cl. 1	cl. 2	cl. 3	**p<0.000001**	cl. 1	cl. 2	cl. 3	**p<0.0001**	cl. 1	cl. 2	cl. 3
	cl. 1		🟩	🟩	cl. 1		🟩	🟩	cl. 1		🟩	🟩
	cl. 2	🟩		🟩	cl. 2	🟩		🟩	cl. 2	🟩		🟩
	cl. 3	🟩	🟩		cl. 3	🟩	🟩		cl. 3	🟩	🟩	
2019_04_15	**p<0.000001**	cl. 1	cl. 2	cl. 3	**p<0.000001**	cl. 1	cl. 2	cl. 3	**p<0.0001**	cl. 1	cl. 2	cl. 3
	cl. 1		🟩	🟩	cl. 1		🟩	🟩	cl. 1		🟩	🟩
	cl. 2	🟩		🟩	cl. 2	🟩		🟩	cl. 2	🟩		🟩
	cl. 3	🟩	🟩		cl. 3	🟩	🟩		cl. 3	🟩	🟩	
2019_04_25	**p<0.000001**	cl. 1	cl. 2	cl. 3	**p<0.000001**	cl. 1	cl. 2	cl. 3	**p<0.0001**	cl. 1	cl. 2	cl. 3
	cl. 1		🟩	🟩	cl. 1		🟩	🟩	cl. 1		🟩	🟩
	cl. 2	🟩		🟩	cl. 2	🟩		🟩	cl. 2	🟩		🟩
	cl. 3	🟩	🟩		cl. 3	🟩	🟩		cl. 3	🟩	🟩	
2019_06_09	**p=0. 02965**	cl. 1	cl. 2	cl. 3	**p=0.720637**	cl. 1	cl. 2	cl. 3	**p=0.103074**	cl. 1	cl. 2	cl. 3
	cl. 1			🟩	cl. 1				cl. 1			
	cl. 2				cl. 2				cl. 2			
	cl. 3	🟩			cl. 3				cl. 3			
2019_06_14	**p=0.18063**	cl. 1	cl. 2	cl. 3	**p=0.204066**	cl. 1	cl. 2	cl. 3	**p=0.409185**	cl. 1	cl. 2	cl. 3
	cl. 1				cl. 1				cl. 1			
	cl. 2				cl. 2				cl. 2			
	cl. 3				cl. 3				cl. 3			
2019_07_29	**p=0.000002**	cl. 1	cl. 2	cl. 3	**p=0.766655**	cl. 1	cl. 2	cl. 3	**p=0.000041**	cl. 1	cl. 2	cl. 3
	cl. 1			🟩	cl. 1				cl. 1			🟩
	cl. 2			🟩	cl. 2				cl. 2			🟩
	cl. 3	🟩	🟩		cl. 3				cl. 3	🟩	🟩	
2019_08_28	**p<0.000001**	cl. 1	cl. 2	cl. 3	**p=0.662965**	cl. 1	cl. 2	cl. 3	**p<0.000001**	cl. 1	cl. 2	cl. 3
	cl. 1		🟩	🟩	cl. 1				cl. 1		🟩	🟩
	cl. 2	🟩		🟩	cl. 2				cl. 2	🟩		🟩
	cl. 3	🟩	🟩		cl. 3				cl. 3	🟩	🟩	
2019_09_22	**p<0.000001**	cl. 1	cl. 2	cl. 3	**p=0.345758**	cl. 1	cl. 2	cl. 3	**p<0.000001**	cl. 1	cl. 2	cl. 3
	cl. 1		🟩	🟩	cl. 1				cl. 1		🟩	🟩
	cl. 2	🟩		🟩	cl. 2				cl. 2	🟩		🟩
	cl. 3	🟩	🟩		cl. 3				cl. 3	🟩	🟩	
2019_10_12	**p<0.000001**	cl. 1	cl. 2	cl. 3	**p<0.000001**	cl. 1	cl. 2	cl. 3	**p<0.000001**	cl. 1	cl. 2	cl. 3
	cl. 1		🟩	🟩	cl. 1		🟩	🟩	cl. 1		🟩	🟩
	cl. 2	🟩		🟩	cl. 2	🟩		🟩	cl. 2	🟩		🟩
	cl. 3	🟩	🟩		cl. 3	🟩	🟩		cl. 3	🟩	🟩	
2019_10_27	**p<0.000001**	cl. 1	**cl. 2**	**cl. 3**	**p<0.000001**	cl. 1	**cl. 2**	**cl. 3**	**p<0.000001**	cl. 1	**cl. 2**	**cl. 3**
	cl. 1		🟩	🟩	cl. 1		🟩	🟩	cl. 1		🟩	🟩
	cl. 2	🟩		🟩	cl. 2	🟩		🟩	cl. 2	🟩		🟩
	cl. 3	🟩	🟩		cl. 3	🟩	🟩		cl. 3	🟩	🟩	
2019_11_01	p<0.000001	cl. 1	cl. 2	cl. 3	p<0.000001	cl. 1	cl. 2	cl. 3	**p<0.000001**	cl. 1	cl. 2	cl. 3
	cl. 1		🟩	🟩	cl. 1		🟩		cl. 1		🟩	🟩
	cl. 2	🟩		🟩	cl. 2	🟩			cl. 2	🟩		🟩
	cl. 3	🟩	🟩		cl. 3				cl. 3	🟩	🟩	

Table A1 continuation

date		cl. 1	cl. 2	cl. 3		cl. 1	cl. 2	cl. 3		cl. 1	cl. 2	cl. 3
2019_11_16	**p=0.000013**	cl. 1	cl. 2	cl. 3	**p=0.010023**	cl. 1	cl. 2	cl. 3	**p=0.00007**	cl. 1	cl. 2	cl. 3
	cl. 1		█		cl. 1		█		cl. 1		█	█
	cl. 2	█			cl. 2	█			cl. 2	█		
	cl. 3	█			cl. 3				cl. 3	█		
2019_12_06	**p<0.000001**	cl. 1	cl. 2	cl. 3	**p=0.009343**	cl. 1	cl. 2	cl. 3	**p<0.000001**	cl. 1	cl. 2	cl. 3
	cl. 1		█		cl. 1		█		cl. 1		█	
	cl. 2	█			cl. 2	█			cl. 2	█		
	cl. 3	█	█		cl. 3				cl. 3	█		
date	**NDVIre3**				**NDRE**				**SAVI**			
2019_02_19	**p<0.00000111**	cl. 1	cl. 2	cl. 3	**p=0.06113**	cl. 1	cl. 2	cl. 3	**p<0.000001**	cl. 1	cl. 2	cl. 3
	cl. 1		█	█	cl. 1				cl. 1		█	█
	cl. 2	█		█	cl. 2				cl. 2	█		█
	cl. 3	█	█		cl. 3				cl. 3	█	█	
2019_03_31	**p<0.000001**	cl. 1	cl. 2	cl. 3	**p=0.002456**	cl. 1	cl. 2	cl. 3	**p<0.000001**	cl. 1	cl. 2	cl. 3
	cl. 1		█	█	cl. 1		█	█	cl. 1		█	█
	cl. 2	█		█	cl. 2	█			cl. 2	█		█
	cl. 3	█	█		cl. 3	█			cl. 3	█	█	
2019_04_15	**p<0.000001**	cl. 1	cl. 2	cl. 3	**p=0.051698**	cl. 1	cl. 2	cl. 3	**p<0.000001**	cl. 1	cl. 2	cl. 3
	cl. 1		█	█	cl. 1				cl. 1		█	█
	cl. 2	█		█	cl. 2				cl. 2	█		█
	cl. 3	█	█		cl. 3				cl. 3	█	█	
2019_04_25	**p<0.000001**	cl. 1	cl. 2	cl. 3	**p=0.079206**	cl. 1	cl. 2	cl. 3	**p<0.000001**	cl. 1	cl. 2	cl. 3
	cl. 1		█	█	cl. 1				cl. 1		█	█
	cl. 2	█		█	cl. 2				cl. 2	█		█
	cl. 3	█	█		cl. 3				cl. 3	█	█	
2019_06_09	**p=0.012523**	cl. 1	cl. 2	cl. 3	**p<0.000001**	cl. 1	cl. 2	cl. 3	**p=0.008061**	cl. 1	cl. 2	cl. 3
	cl. 1			█	cl. 1		█	█	cl. 1			█
	cl. 2			█	cl. 2	█		█	cl. 2			
	cl. 3	█			cl. 3	█	█		cl. 3	█		
2019_06_14	**p=0.127944**	cl. 1	cl. 2	cl. 3	**p<0.000001**	cl. 1	cl. 2	cl. 3	**p=0.058782**	cl. 1	cl. 2	cl. 3
	cl. 1				cl. 1		█	█	cl. 1			
	cl. 2				cl. 2	█		█	cl. 2			
	cl. 3				cl. 3	█	█		cl. 3			
2019_07_29	**p=0.000001**	cl. 1	cl. 2	cl. 3	**p<0.000001**	cl. 1	cl. 2	cl. 3	**p=0.234653**	cl. 1	cl. 2	cl. 3
	cl. 1			█	cl. 1		█	█	cl. 1			
	cl. 2			█	cl. 2	█		█	cl. 2			
	cl. 3	█	█		cl. 3	█	█		cl. 3			
2019_08_28	**p<0.000001**	cl. 1	cl. 2	cl. 3	**p<0.000001**	cl. 1	cl. 2	cl. 3	**p=0.101259**	cl. 1	cl. 2	cl. 3
	cl. 1		█	█	cl. 1		█	█	cl. 1			
	cl. 2	█		█	cl. 2	█		█	cl. 2			
	cl. 3	█	█		cl. 3	█	█		cl. 3			
2019_09_22	**p<0.000001**	cl. 1	cl. 2	cl. 3	**p<0.000001**	cl. 1	cl. 2	cl. 3	**p=0.312013**	cl. 1	cl. 2	cl. 3
	cl. 1		█	█	cl. 1		█	█	cl. 1			
	cl. 2	█		█	cl. 2	█		█	cl. 2			
	cl. 3	█	█		cl. 3	█	█		cl. 3			
2019_10_12	**p<0.000001**	cl. 1	cl. 2	cl. 3	**p<0.000001**	cl. 1	cl. 2	cl. 3	**p=0.000017**	cl. 1	cl. 2	cl. 3
	cl. 1		█	█	cl. 1		█	█	cl. 1			█
	cl. 2	█		█	cl. 2	█			cl. 2			█
	cl. 3	█	█		cl. 3	█			cl. 3	█	█	
2019_10_27	**p<0.000001**	cl. 1	cl. 2	cl. 3	**p=0.015262**	cl. 1	cl. 2	cl. 3	**p=0.000002**	cl. 1	cl. 2	cl. 3
	cl. 1		█	█	cl. 1			█	cl. 1			█
	cl. 2	█		█	cl. 2				cl. 2			█
	cl. 3	█	█		cl. 3	█			cl. 3	█	█	

Table A1 continuation

2019_11_01	**p<0.000001**	cl. 1	cl. 2	cl. 3	**p=0.003243**	cl. 1	cl. 2	cl. 3	**p=0.000001**	cl. 1	**cl. 2**	**cl. 3**
	cl. 1		■	■	cl. 1			■	cl. 1			■
	cl. 2	■		■	cl. 2				cl. 2			■
	cl. 3	■	■		cl. 3	■			cl. 3	■	■	
2019_11_16	**p=0.000021**	cl. 1	cl. 2	cl. 3	**p=0.02236**	cl. 1	cl. 2	cl. 3	**p=0.000285**	cl. 1	**cl. 2**	**cl. 3**
	cl. 1		■	■	cl. 1			■	cl. 1			■
	cl. 2	■			cl. 2				cl. 2			
	cl. 3	■			cl. 3	■			cl. 3	■		
2019_12_06	**p<0.000001**	cl. 1	cl. 2	cl. 3	**p=0.000372**	cl. 1	cl. 2	cl. 3	**p=0.000065**	cl. 1	**cl. 2**	**cl. 3**
	cl. 1		■	■	cl. 1			■	cl. 1			■
	cl. 2	■			cl. 2			■	cl. 2			■
	cl. 3	■			cl. 3	■	■		cl. 3	■	■	

date	GNDVI				EVI			
2019_02_19	**p<0.000001**	cl. 1	cl. 2	cl. 3	**p<0.000001**	cl. 1	cl. 2	cl. 3
	cl. 1		■	■	cl. 1		■	■
	cl. 2	■		■	**cl. 2**	■		■
	cl. 3	■	■		**cl. 3**	■	■	
2019_03_31	**p<0.000001**	cl. 1	cl. 2	cl. 3	**p<0.000001**	cl. 1	cl. 2	cl. 3
	cl. 1		■	■	cl. 1		■	■
	cl. 2	■		■	**cl. 2**	■		■
	cl. 3	■	■		**cl. 3**	■	■	
2019_04_15	**p<0.000001**	cl. 1	cl. 2	cl. 3	**p<0.000001**	cl. 1	cl. 2	cl. 3
	cl. 1		■		cl. 1			■
	cl. 2	■		■	cl. 2			■
	cl. 3	■	■		cl. 3	■	■	
2019_04_25	**p<0.000001**	cl. 1	cl. 2	cl. 3	**p=0.079206**	cl. 1	cl. 2	cl. 3
	cl. 1		■		cl. 1			■
	cl. 2	■		■	cl. 2			■
	cl. 3	■	■		cl. 3	■	■	
2019_06_09	**p<0.000001**	cl. 1	cl. 2	cl. 3	**p=0.001828**	cl. 1	cl. 2	cl. 3
	cl. 1			■	cl. 1			■
	cl. 2			■	cl. 2			■
	cl. 3	■	■		cl. 3	■	■	
2019_06_14	**p<0.000001**	cl. 1	cl. 2	cl. 3	**p=0.026929**	cl. 1	cl. 2	cl. 3
	cl. 1			■	cl. 1			■
	cl. 2			■	cl. 2			
	cl. 3	■	■		cl. 3	■		
2019_07_29	**p<0.000001**	cl. 1	cl. 2	cl. 3	**p=0.306634**	cl. 1	cl. 2	cl. 3
	cl. 1		■	■	cl. 1			
	cl. 2	■		■	cl. 2			
	cl. 3	■	■		cl. 3			
2019_08_28	**p<0.000001**	cl. 1	cl. 2	cl. 3	**p=0.144126**	cl. 1	cl. 2	cl. 3
	cl. 1		■	■	cl. 1			
	cl. 2	■		■	cl. 2			
	cl. 3	■	■		cl. 3			
2019_09_22	**p<0.000001**	cl. 1	cl. 2	cl. 3	**p=0.558712**	cl. 1	cl. 2	cl. 3
	cl. 1		■	■	cl. 1			
	cl. 2	■		■	cl. 2			
	cl. 3	■	■		cl. 3			

Table A1 continuation

	p<0.000001	cl. 1	cl. 2	cl. 3	p=0.000087	cl. 1	cl. 2	cl. 3
2019_10_12	cl. 1		■	■	cl. 1			■
	cl. 2	■		■	cl. 2			■
	cl. 3	■	■		cl. 3	■	■	
	p<0.000001	cl. 1	cl. 2	cl. 3	p=0.00001	cl. 1	cl. 2	cl. 3
2019_10_27	cl. 1		■	■	cl. 1			■
	cl. 2	■		■	cl. 2			■
	cl. 3	■	■		cl. 3	■	■	
	p<0.000001	cl. 1	cl. 2	cl. 3	p=0.000003	cl. 1	cl. 2	cl. 3
2019_11_01	cl. 1		■	■	cl. 1			■
	cl. 2	■		■	cl. 2			■
	cl. 3	■	■		cl. 3	■	■	
	p<0.000001	cl. 1	cl. 2	cl. 3	p=0.000704	cl. 1	cl. 2	cl. 3
2019_11_16	cl. 1		■	■	cl. 1			■
	cl. 2	■			cl. 2			
	cl. 3	■			cl. 3	■		
	p<0.000001	cl. 1	cl. 2	cl. 3	p=0.000075	cl. 1	cl. 2	cl. 3
2019_12_06	cl. 1		■	■	cl. 1			■
	cl. 2	■		■	cl. 2			■
	cl. 3	■	■		cl. 3	■	■	
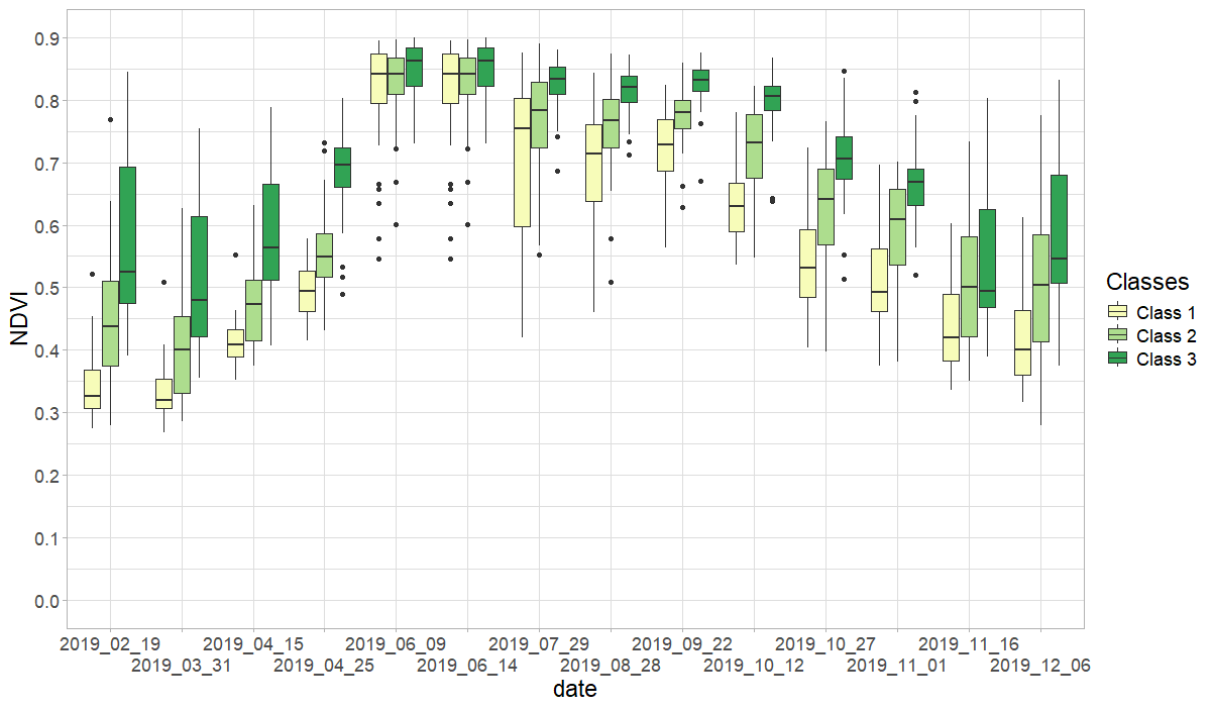
Figure A 1. Distribution of NDVI values for three classes of natural succession in the growing season. Box plot description see Figure 4.
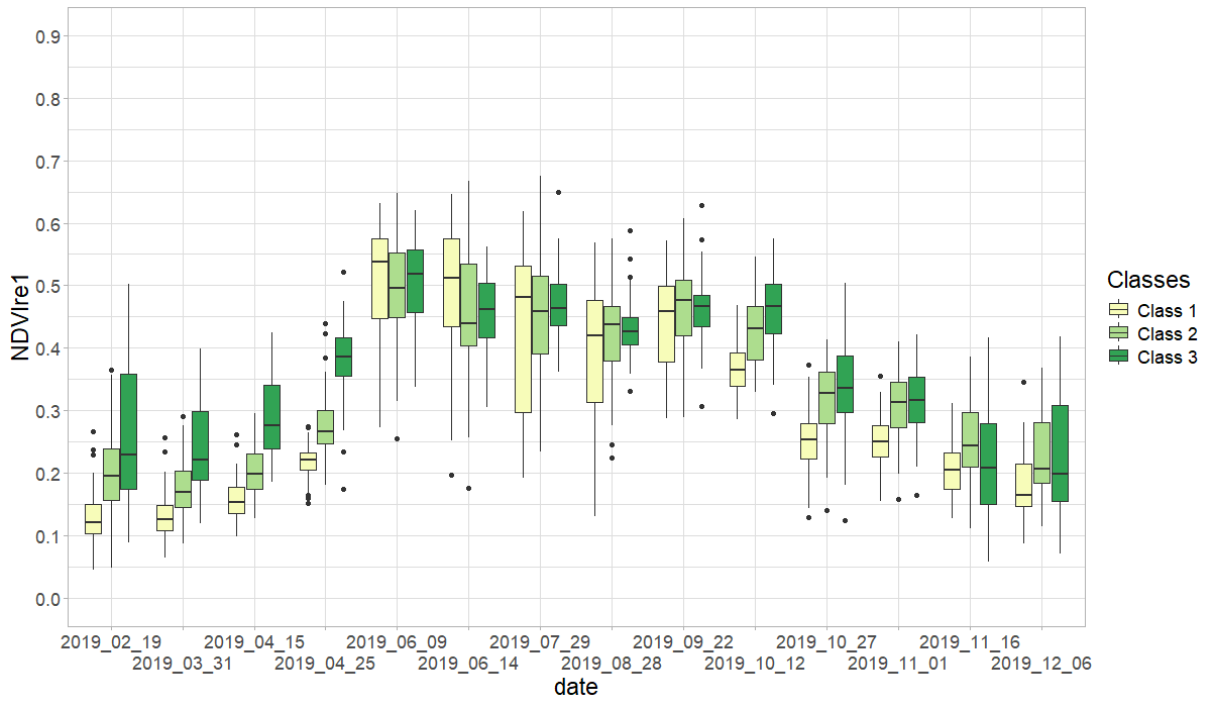
Figure A 2. Distribution of NDVIre1 values for three classes of natural succession in the growing season. Box plot description see Figure 4.
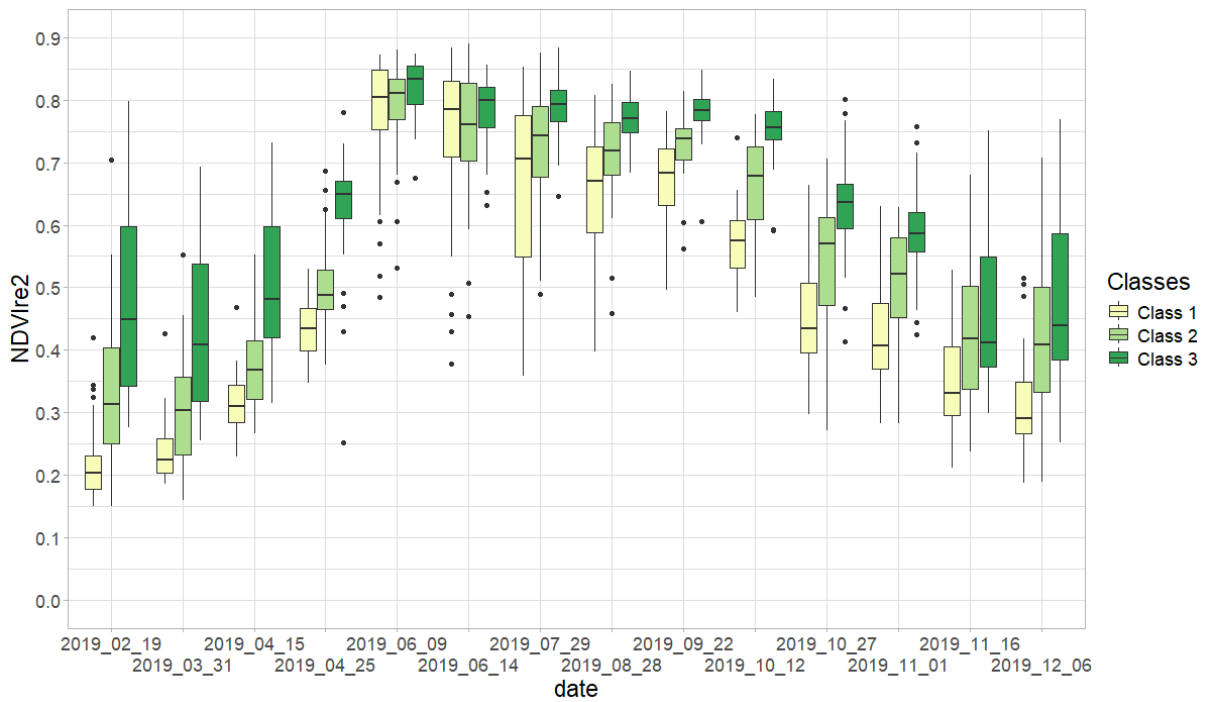

Figure A 3. Distribution of NDVIre2 values for three classes of natural succession in the growing season. Box plot description see Figure 4.
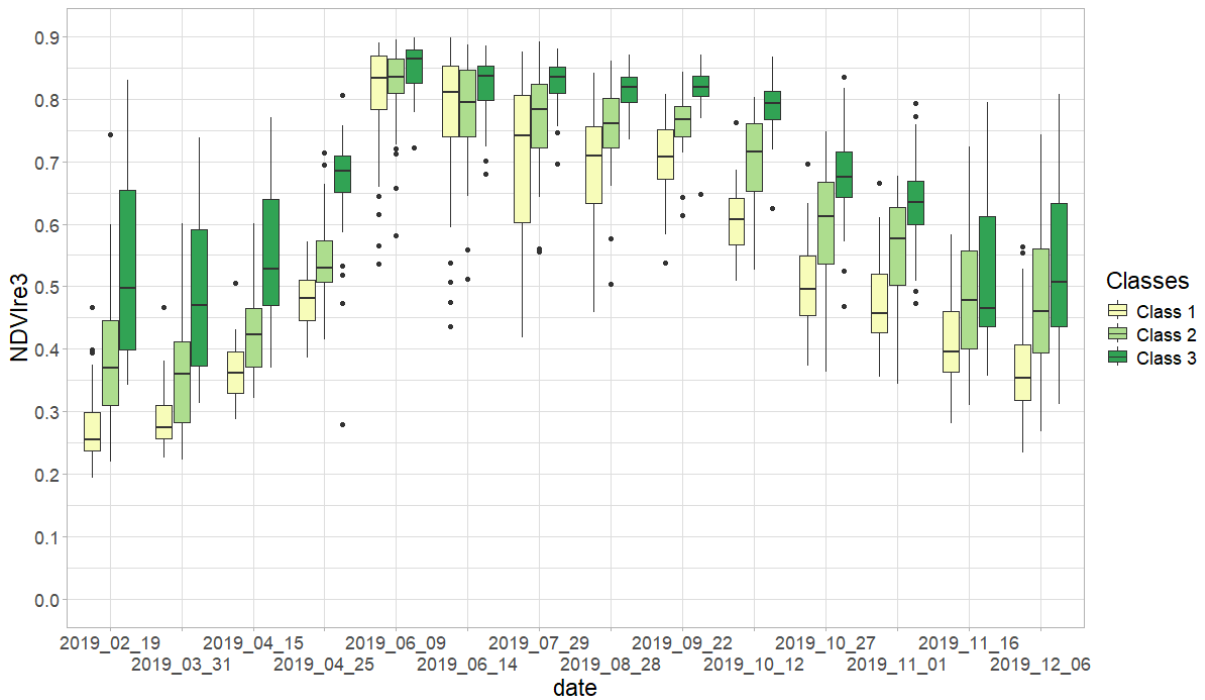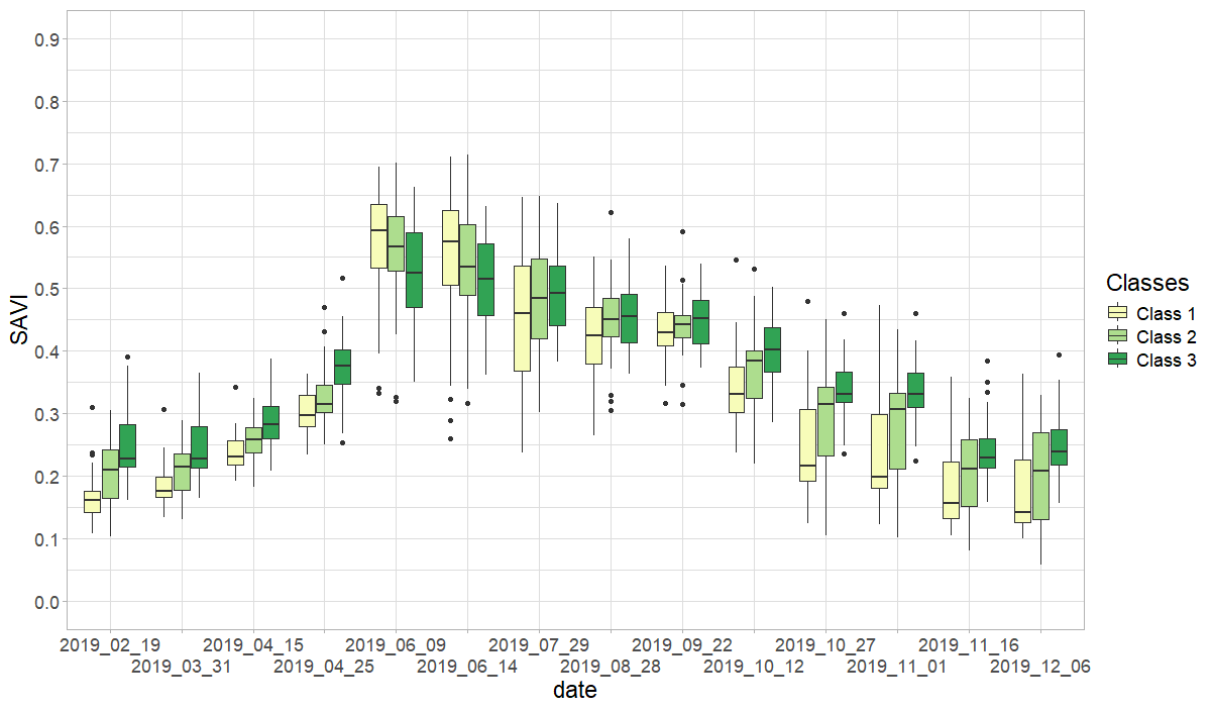
Figure A 4. Distribution of NDVIre3 values for three classes of natural succession in the growing season. Box plot description see Figure 4.

Figure A 5. Distribution of SAVI values for three classes of natural succession in the growing season. Box plot description see Figure 4.
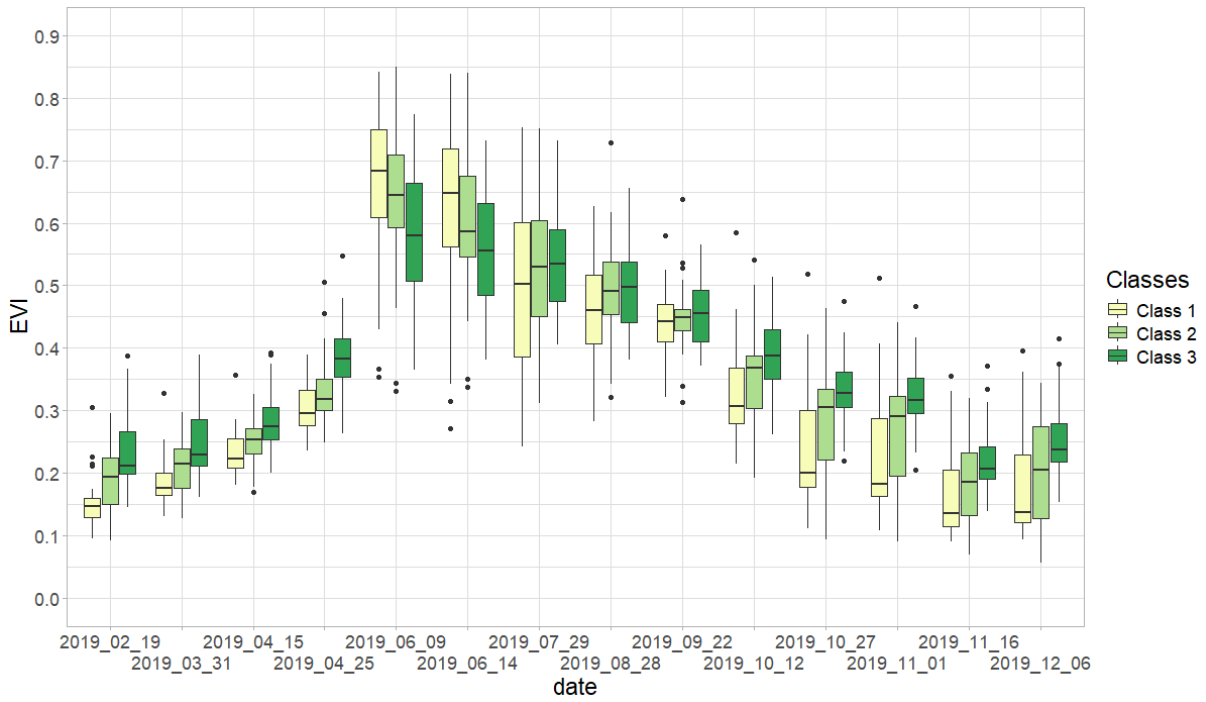
Figure A 6. Distribution of EVI values for three classes of natural succession in the growing season. Box plot description see Figure 4.
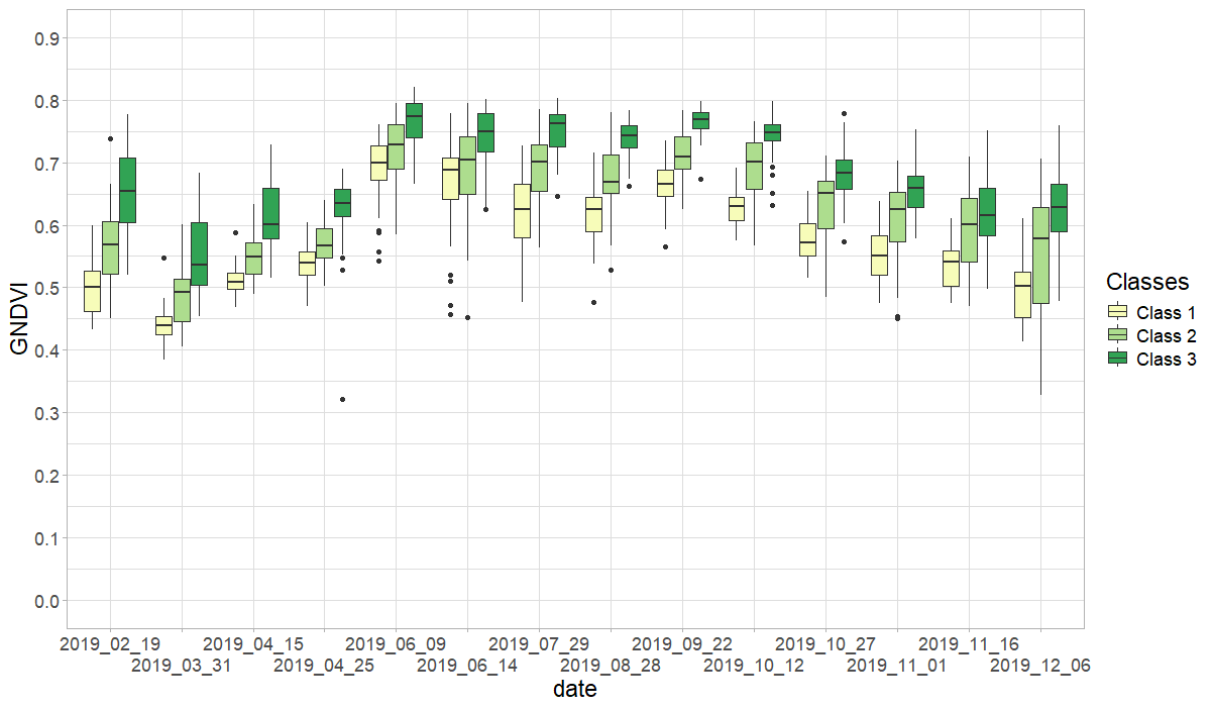

Figure A 7. Distribution of GNDVI values for three classes of natural succession in the growing season. Box plot description see Figure 4.

Figure A 8. Distribution of NDRE values for three classes of natural succession in the growing season. Box plot description see Figure 4.